Measurements of Film Flow Rate in Heated Tubes with Various Axial Power Distributions

by

Carl Adamsson

February 2006
Technical Reports from
Royal Institute of Technology
KTH Nuclear Reactor Technology
SE-106 91 Stockholm, Sweden

Akademisk avhandling som med tillstånd av Kungliga Tekniska Högskolan i Stockholm framlägges till offentlig granskning för avläggande av teknologie licentiatexamen måndagen den 13 Mars 2006 kl 10.15 i Seminarierum 112:028, Reaktorteknologi, Alba Nova, Roslagtullsbacken 11, Stockholm.

Universitetsservice US–AB, Stockholm 2006

Carl Adamsson 2006, **Measurements of Film Flow Rate in Heated Tubes with Various Axial Power Distributions**

KTH Nuclear Reactor Technology, SE-106 91 Stockholm, Sweden

Abstract

Measurements of film mass flow rate for annular, diabatic steam-water flow in tubes are presented. The measurements were carried out with four axial power distributions and at several axial positions at conditions typical for boiling water reactors, i.e. 7 MPa pressure and total mass flux in a range from 750 to 1750 kg/m^2s. The results show that the influence of the axial power distribution on the dryout power corresponds to a consistent tendency in the film flow rate and that the film tends to zero when dryout is approached. Furthermore it is demonstrated that two selected phenomenological models of annular flow well predict the present data. A model for additional entrainment due to boiling is shown to degrade the predictions.

Descriptors: film flow, film thickness, dryout, power distribution, annular flow

Preface

This thesis consists of two parts. The first is an introduction and summary of the present work that provides some background and overview as well as summarizes the main results and conclusions. The second part consists of three published papers, which have been adjusted to comply with the format of the thesis, but have not been changed except for minor refinements.

December 2005, Stockholm
Carl Adamsson

Contents

Part I

Overview and summary

CHAPTER 1

Introduction

1.1. Background

In many boiling systems, and in particular in water cooled nuclear reactors, the maximal possible power is limited by a phenomenon called critical heat flux (CHF). It appears as a sudden detoriation of the heat transfer process when the power exceeds a certain limit, which causes a sharp rise in the heater temperature that is likely to destroy the heater. It is obvious that measures must be taken to prevent CHF from occurring, either by limiting the power or by optimizing the construction in order to increase the margins to CHF. In either case accurate methods to predict the phenomenon are needed.

The CHF phenomenon is not easy to define in general terms, but if the discussion is limited to steady-state heat flux controlled systems, the following definition will be satisfactory:

> The critical heat flux is the heat flux at which further increase of the power will result in a sudden increase of the heater temperature.

This definition is based on how the CHF phenomenon is usually measured and not on the underlying mechanism that caused it. In fact, there are several different mechanisms that may give rise to a rapid wall temperature increase. Thus, the definition above does not really refer to one phenomenon but rather to a whole class of related phenomena, which will occur in many types of boiling systems. This thesis, however, is concerned only with the type of CHF that typically occurs in boiling water nuclear reactors (BWR) and is usually termed dryout. In pressurized water reactors (PWR) another phenomenon occurs that fits the CHF definition given above. It is usually called departure from nucleate boiling (DNB) and the mechanism is different from that of dryout. The DNB phenomenon will not be further considered in this thesis. It is just noted here that DNB typically occurs when the bulk liquid is subcooled through the formation of a thin vapor film at the heated surface. Dryout, on the other hand, is associated with the annular flow regime. That is, the vapor phase forms the core of the flow while the liquid travels partly as a liquid film on the walls and partly as drops entrained in the vapor. Dryout occurs when the liquid film is no longer able to wet the wall.

A large amount of work, over several decades, has been spent on understanding how the dryout phenomenon arises. Today the fundamental mechanisms are, at least qualitatively, well understood, but some questions remain open. It is generally agreed upon that dryout occurs when the liquid film is no longer able to efficiently wet the wall so that heat, instead of evaporating the film, must be transported away from the wall by significantly less efficient forced convection to vapor. It is also clear that deposition of entrained drops to the film and mechanical entrainment of film into drops are highly crucial mechanisms. What is less clear is whether the film thickness will go continuously to zero as the dryout power is approached or if there is a critical film thickness where the film, for one reason or another, will suddenly break up and dryout occur. Experiments by Milashenko *et al.* (1989) and Ueda & Isayama (1981) indicate significant critical film thickness, while experiments by Hewitt *et al.* (1965) and, as will be shown, the present experiments imply that it is negligible. This discrepancy is most likely due to the fact that the first two experiments, which showed critical film, were performed in much shorter tubes (around 1 m) and correspondingly higher heat fluxes than the latter. This only confirms that dryout changes into a different phenomenon (DNB) at low steam quality.

Another interesting and not fully settled question is that of the role of the heat flux (apart from the obvious effect as the source of evaporation). It has sometimes been treated as the main parameter controlling the CHF phenomenon, which is evident from the name critical heat flux itself as well as from the traditional way of constructing dryout correlations (see chapter 3.1). Experiments by Groeneveld (1975) with a 'flux spike', however, showed that at low steam quality the onset of CHF indeed follows the local heat flux but at high steam quality the the spike had almost no effect with the mean flux instead controlling the dryout. Again this confirms that CHF is different at low respective high steam quality but also shows that the use of the local heat flux in dryout models is not straight forward. It has been argued that the rate of entrainment depends strongly on the heat flux (Milashenko *et al.* 1989), while other models have been constructed with no such influence at all (Hewitt & Govan 1990). Yet other models have mixed the two approaches, see e.g. Hoyer (1998) and Okawa *et al.* (2003).

The discussion in the previous paragraph leads directly to that of the influence of the power distribution. For it is so that, even if the local heat flux is not directly controlling the dryout phenomenon, neither is the mean heat flux along the channel enough. On the contrary it is well known that shifting the power towards the outlet, where the steam quality is high, will decrease the dryout power, while shifting it towards the inlet will increase the power at which dryout occurs. (See e.g. Blomstrand *et al.* (2000))

The mechanism behind this behavior was qualitatively explained by an elegant series of experiments by Bennett *et al.* (1966). They measured the film

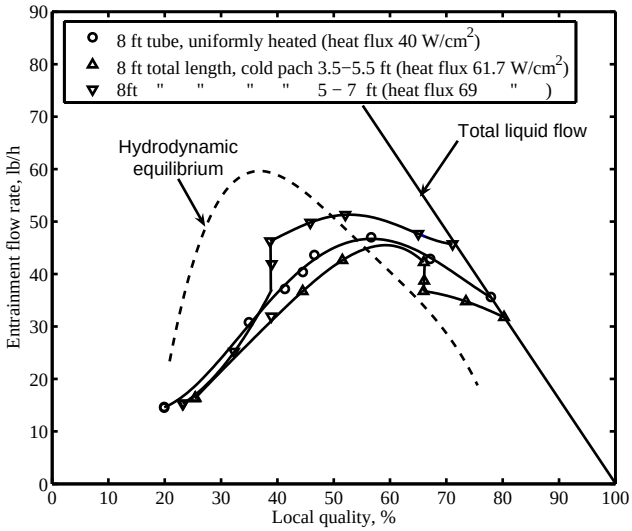

FIGURE 1.1. Reproduced from Bennett *et al.* (1966)

flow rate in a heated pipe, where the power profile contained moveable cold patches. Strikingly it was possible to achieve higher dryout power with a cold patch close to the outlet than with a completely uniform power distribution.

The mechanism is most readily explained with help of Figure 1.1 that is reproduced from the original paper. The figure shows the flow rate of entrained drops against the steam quality for different placements of the cold patch together with the hydrodynamic equilibrium curve (from measurements in very long adiabatic pipes). At the cold patches the entrained drop curve tends towards the equilibrium curve. When the cold patch is close to the inlet this leads to an increased drop flow rate and thus a reduction in the dryout steam quality. When the cold patch is close to the outlet, on the other hand, the tendency towards equilibrium will reduce the amount of drops and increase the dryout steam quality. Dryout is here supposed to occur when the entrained drop curve meets the total liquid line, i.e. when the film flow rate is zero.

1.2. Objectives

The objective of the present work is primarily to confirm the findings by Bennett *et al.* (1966) for several realistic power distributions at conditions typically found in a BWR and to extend the database of film measurements that can be used for direct validation of phenomenological models of annular two-phase flow.

To study the phenomena of deposition and entrainment it is almost necessary to have information about axial development of the liquid film. This means that a single measurement of the film close to the channel exit is not enough. The present experimental program therefore includes measurements at several axial positions for each power distribution.

Since the high-pressure two-phase loop was not equipped with the measurement system needed for this type of experiments, it had to be constructed (see Chapter 2). In order to simplify the necessary installations and to be able to study one pure physical effect, the experiments were carried out in the simplest possible geometry, i.e. a round tube without any spacer grids or other obstacles. The influence of the power distribution is rather weak in such a system compared to more complex geometrical configurations with spacer grids, but the simplicity of the measurement system and the analysis that could be achieved nevertheless made this choice preferable.

CHAPTER 2

Experimental Techniques

2.1. Earlier Experiments

Since dryout is triggered by the disappearance of the liquid film from the heated surface, the key to understanding the phenomenon is accurate measurements of the film. For this purpose one could measure either the thickness of the film or the film mass flow rate. The thickness has been measured with needle probes (Würtz 1978) and conductance probes (Collier & Hewitt 1964). These techniques are fast and make it possible to measure not only the average film thickness but also the waves traveling with the film. In dryout modeling, however, it is usually the mass flow rate that turns up in the equations, since this parameter can easily be related to the mass- and energy balances. For that reason it was decided to measure the film mass flow rate in this project.

A technique to do that by extracting the liquid film through the wall of the test-section has been shown to be reliable by several studies before. The idea is to slowly increase the extraction rate from a low value and at each step measure the amounts of liquid and gas in the sample. (In air-water systems this can be done with a separator, for steam-water systems the most reliable method is to condense the sample and rely on the heat balance as described below). When the flow of liquid no longer increases as the extraction rate is increased, it is assumed that the film flow rate has been found.

The earliest such experiments were performed on air-water systems and a slit in the wall was used to extract the film (Bennett & Thornton 1961). Since large waves in the film tend to overshoot the slit, it was replaced by a porous wall section in later studies. Hewitt *et al.* (1965) and Hewitt & Pulling (1969) used sinter metal wall sections and Würtz (1978) used a 5 cm wall section perforated with 1.2 mm holes. Singh *et al.* (1969) studied the influence of the length of the porous wall section and concluded that waves will overshoot if it is too short. On the other hand, if it is too long the measurements will be inaccurate. It was recommended to use a length of 1 in. In accordance with this recommendation, the present study used a 30 mm sinter metal wall section (with effective length slightly shorter).

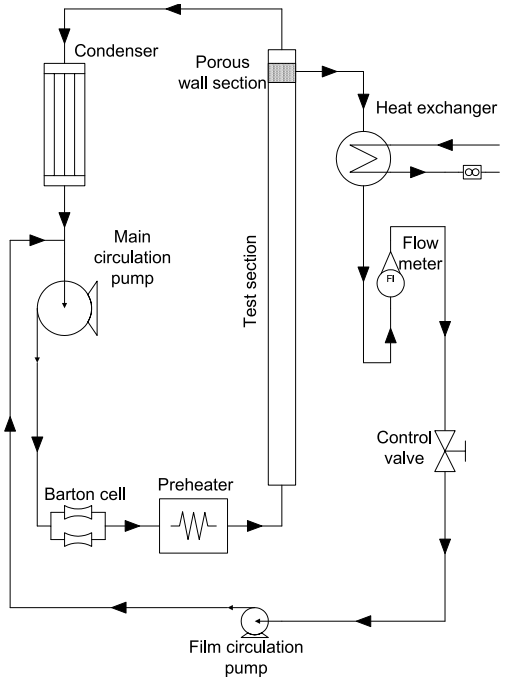

FIGURE 2.1. Working principles of the main loop and the film extraction loop.

2.2. Present Experimental Setup

The working principle of the main loop and the film measurement system is shown in Figure 2.1. Before the test-section, the water passed through a 150 kW preheater to achieve the desired inlet temperature. The test-sections were manufactured from 3.65 m long stainless steel pipes with 14 mm inner diameter and were heated by an electric current (DC) in the steel. The power was calculated as the product of this current and the voltage over the test-section and the power distribution was imposed by letting the outer diameter of the pipe vary (thereby varying the electrical resistance).

The power distributions that were studied in the present work are shown in Figure 2.2 and Table 1 in Appendix A. (The power distributions shown are the actual power distributions obtained by measuring the local electrical resistance of the test-sections). These four distributions – the uniform, inlet peaked, middle peaked and outlet peaked – were chosen to be able to study the well documented effect of decreasing dryout power when the power peak

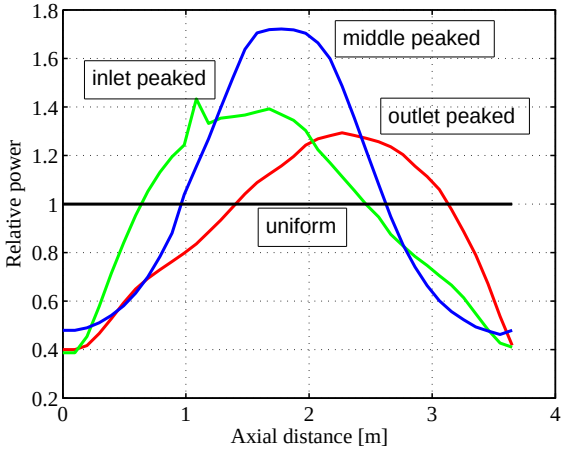

FIGURE 2.2. The four axial power distributions used in the experiments. The spike in the inlet peaked distribution is a manufacturing fault.

moves towards the exit and since a large amount of dryout data are available for these distributions.

The water was then condensed before it passed through the main circulation pump and the flow measurement system, which consisted of four 1000 mm long pipes with various diameters. The flow rate measurements were based on measuring the pressure drop over one of these pipes with a Barton cell.

To this was added the film extraction loop with a heat exchanger, flow meter and a second circulation pump. The purpose of the heat exchanger was to condense the extracted sample before it entered the flow mater. The vapor content could then be calculated by monitoring the temperatures and flow rates at the primary and secondary sides of the heat exchanger. These calculations, which were carried out automatically by a LABVIEW software during the measurements, are described in detail in Paper 3.

The results were analyzed graphically by plotting the extracted liquid flow rate against the vapor fraction in the sample to obtain an L-shaped curve as shown in Figure 2.5. The film flow rate could be read off as the intersection of the vertical part of the curve with the horizontal axis. (For details about the analysis of the extraction curves and more examples, see Paper 1 and Paper 3).

Figures 2.3 and 2.4 show photographs of the film extraction device and the sinter metal section that was used in the experiments. Note the small distance between the power clamp to the right in Figure 2.3 and the extraction point. It

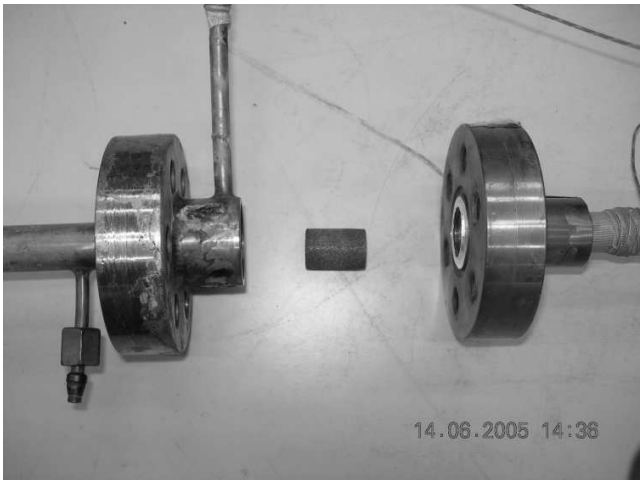

FIGURE 2.3. Side view of dismounted film extraction device.

FIGURE 2.4. The porous sinter metal part mounted in the film extraction device.

is important to have this distance as small as possible to prevent redeposition of drops before the measurement point.

The heat exchanger was placed as close as possible to the extraction point and was well insulated to prevent heat losses in the connection pipe. Several thermocouples were used to measure the various temperatures at the primary

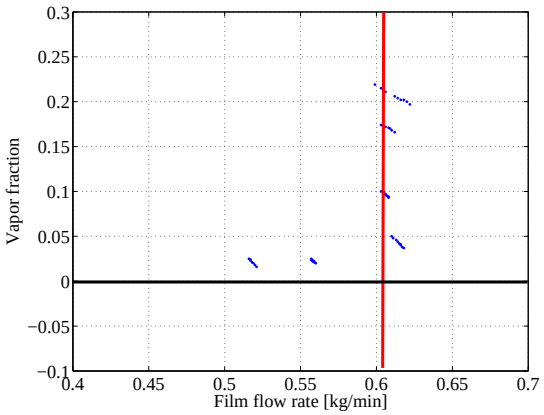

FIGURE 2.5. Example of suction curve from the experiments. The film flow rate is determined from the intersection of the vertical part of the curve with the horizontal axis.

and secondary sides. This redundancy in the temperature measurements made it easier to estimate the accuracy (see Chapter 2.4).

2.3. Measurement Procedure

For each experiment the first step was to establish steady-state in the main loop at the desired conditions. The sample flow rate through the porous wall was then adjusted to a low value (compared to the expected film flow rate). After a couple of minutes a steady-state had developed in the main loop and the heat exchanger in the film extraction loop. (The LABVIEW software used had functions to help the operators maintain the steady-state during the measurements). All monitored parameters of the system were then saved, the sample flow rate was increased and a new steady-state was allowed establish itself. This continued until as much as possible of the expected L-shaped curve was obtained, which could usually be accomplished within half an hour.

The use of stainless steel implied that the test-section could not withstand post-dryout conditions (other options were considered but ruled out for practical reasons). Hence all experiments had to be performed with some margin to the dryout condition. The procedure used was to start each series of measurements by finding the dryout power at the corresponding flow rate. The steam quality was then reduced by approximately 3% and the film flow measurements started from that lower power. A second series of measurements was also carried out at approximately 10% reduced power. (The full matrix of experiments can be found in Paper 3).

For the uniform power distribution the effective axial position of the filter was changed by changing the inlet temperature, thereby moving the onset of

boiling without changing the heat flux. This procedure is however not possible for the non-uniform distributions. In these cases the test-sections had to be dismounted, cut and reassembled again.

After this operation the power to the test-section must be adjusted to reproduce the local heat flux (as opposed to the mean). To achieve this, the local heat flux was measured by monitoring the voltage over a short section of the test-section close to the inlet. The local power could then be calculated as the product of this voltage and the current in the test-section.

2.4. Accuracy

The accuracy of the results from measurements is naturally an issue of major importance. The errors that will always be present in any experimental data can be divided in two types – random uncertainties and systematic errors. The random part is caused by the uncertainty of the instrumentation and can relatively easily be analyzed. The systematic errors are due to possible physical effects that were not considered in the analysis of the data. Examples that should be considered are heat losses in the equipment, consequences of waves on the film surface and redepositon of entrained drops before the extraction point.

A thorough analysis of both the random uncertainties and systematic errors can be found in Paper 3. It was concluded that the main source of uncertainties was the flow measurements in the film loop. In the present project a rotameter from KROHNE was used for this purpose. It was calibrated to be accurate within 2% for flow rates between 0.3 and 3.0 kg/min. When the measured film flow rate was small this accuracy was not fully satisfactory and at the end of the project the equipment was complemented with an addition flow meter of turbine type, calibrated for low flow rates. It proved to be more reliable than the rotameter and it is hence recommended to replace the rotameter with a turbine flow meter in future measurements.

It was also concluded in Paper 3 that heat losses in the extraction loop and redeposition of drops were small enough to be neglected. The interpretation of the suction curves, however, sometimes constitutes a significant error source. More examples of exctraction curves can be found in Paper 1 and Paper 3 and it is clear from the figures there that not all the curves had the ideal L-shape shown in Figure 2.5. Sometimes the deviation could be explained by disturbance waves on the film surface, but in other cases it must be treated as an uncertainty of the measurement equipment. (See Paper 3 for examples and a more detailed discussion of this issue).

Finally it was estimated that measurements with reasonably sharp and readily interpreted suction curves could be considered to be accurate within ± 0.1 kg/min and measurements with distorted suction curves were considered

accurate within ± 0.2 kg/min. All error bars shown in this thesis are based on that estimate.

CHAPTER 3

Models and Correlations

3.1. Dryout Correlations

Even though a lot of work has been done to formulate accurate models of the dryout phenomenon, the method that is most commonly used in practice is empirical correlations (or lookup tables). In this section the theoretical basis for such methods is outlined in order to conclude when they should be used and when they can be expected to fail.

The system analyzed here is a general, vertical channel of any geometry (tube, annulus, rod bundle or other) with upwards flowing boiling water and heat applied through one or more walls. Furthermore it is assumed that the system operates under steady-state conditions. The discussions will also be limited to the case when the inlet is subcooled for reasons explained below.

Now define a set of parameters – or boundary conditions – that can be assumed to completely define the state of the system for a fixed geometry. The state here refers to all aspects of the system in which we have any interest, in particular whether any part of the heated surface is in dryout or not. One such set of boundary conditions consists of:

- inlet mass flux (G)
- inlet enthalpy (h_{in})
- outlet pressure (p)
- average heat flux ($\overline{q''}$)
- channel length (L)

Note that these parameters are easily defined in terms of single numbers. The reason to assume a subcooled inlet is that if a two-phase mixture were introduced at the inlet the conditions there would have to be specified in more detail.

There is one additional parameter – the power distribution. It can be defined as a function that to each part of the wetted wall assigns a relative heat flux, i.e. the ratio of the local heat flux to the average heat flux. The power distribution can obviously not be described with a single number. With the assumption that the five parameters above (assuming constant, but not necessarely uniform power distribution) completely define the state of the system and given a large enough matrix of dryout experiments on this geometry it is

possible to construct a four dimensional lookup-table of the critical heat flux or, alternatively, to fit a mathematical function in four variables to the data.

Considering the physics it is, however, possible to introduce additional simplifying assumptions. Since the inlet is subcooled there will be single-phase flow in the lowest part of the channel. In this part it may be assumed that the conditions are completely described by the mass flux and the fluid enthalpy. (Note that this would not be true for phenomena such as DNB or subcooled boiling, but here only dryout at high steam quality is considered). With this assumption a new (artificial) inlet could be defined anywhere in the subcooled region and in particular at the onset of boiling, where the enthalpy can be assumed to be that of saturation at the given pressure and thus be omitted as a boundary condition.

In this way the defining set is reduced to:

- inlet mass flux (G)
- outlet pressure (p)
- average heat flux ($\overline{q''}$)
- boiling length (L_b)

From these parameters the (equilibrium) outlet steam quality may be calculated and, if so prefered, replace any one of the parameters in the defining set. Replacing the boiling length with the outlet steam quality gives the classical heat flux/steam quality correlation form (see Hewitt in Hetsroni (1982)). Note that it is the average heat flux and outlet steam quality that appears in the correlation as it was derived here, not the local values. Replacing the heat flux in the defining set with the steam quality gives another classical correlation form: the steam quality/boiling length. It is clear from the argument here that the two forms are completely equivalent. That is, as long as the power profile is kept constant (but not necessarily uniform), which is a fundamental assumption for the reasoning in this chapter and thus the weakness of all dryout correlations.

Thus it can be concluded that empirical correlations can be expected to work if only a limited number of parameters, which are possible to describe with single numbers, are varied and enough data for calibration are available. When parameters are varied that can not be described with single numbers, such as the geometry or the power distribution, the correlation concept will most possibly fail. In such cases, and when there are not enough data to calibrate a correlation properly, models built on physical reasoning must be considered.

3.2. Phenomenological Models

Many models of annular flow with the aim to predict the dryout power have been formulated. Most of them are built on the assumption that annular flow in one dimension can be described as a vapor core with entrained liquid drops and a liquid film on the wall and that three main mass transfer mechanism are

working: evaporation of film into vapor, deposition of drops that become film and entrainment of film into drops. The simplest models are based only on the mass conservation for the liquid film, which can be written as:

$$\frac{1}{P}\frac{dW_f}{dz} = D - E - \Gamma \tag{3.1}$$

where W_f denotes the liquid film flow rate, P is the wall perimeter and D, E and Γ are the deposition rate, entrainment rate and evaporation rate respectively. The evaporation rate can easily be calculated from the wall heat flux, but for the deposition and entrainment processes, empirical or semi-empirical correlations are usually used.

Equation 3.1 must be equipped with an appropriate boundary condition. Since the equation can be expected to describe the flow only when the flow regime is annular, it is natural to impose the boundary condition at the beginning of annular flow. Thus, in addition to models for the deposition and entrainment rates a model for the onset of annular flow and the film flow rate there is necessary. For very long channels (more than 6–7 m) the boundary condition is not particularly important, but in the present case it is of crucial importance for the model.

3.3. Deposition Models

Most models for the deposition of drops to the walls are based on the assumption that the phenomenon is caused by a diffusion like mechanism. It is then natural to assume that the deposition rate should be related to the concentration of drops in the vapor core. It is therefore common to introduce a deposition velocity, k_d, as:

$$D = k_d C \tag{3.2}$$

where C is the effective drop density in the vapor core. A large number of empirical correlations for k_d have been published. Hewitt & Govan (1990) proposed the following expression:

$$k_d = 0.083 \max\left(0.3, \frac{C}{\rho_v}\right)^{-0.65} \sqrt{\frac{\sigma}{\rho_v d_h}} \tag{3.3}$$

which was modified by Okawa *et al.* (2003) to read

$$k_d = 0.0632 \left(\frac{C}{\rho_v}\right)^{-0.5} \sqrt{\frac{\sigma}{\rho_v d_h}} \tag{3.4}$$

Other correlations are, for example, due to Sugawara (1990), de Bertodano & Assad (1998) and Utsuno & Kaminaga (1998).

3.4. Entrainment Models

For entrainment models the diversity is larger. Since the entrainment rate is very difficult to measure, the only data that is available is for hydrodynamic equilibrium, where $D = E$, so that the entrainment rate is given by the deposition correlation. Many entrainment correlations are therefore return-to-equilibrium models, based on the assumption $E = k_d C_{eq}$, where the effective drop concentration at equilibrium, C_{eq}, is correlated. With this approach it is, however, easy to get unphysical models, since correlations for C_{eq} are usually not given in the relevant local parameters.

The entrainment process is highly complex and all details are not well understood, but there are correlations with more physically plausible form than the simple return-to-equilibrium. For example, Hewitt & Govan (1990), proposed

$$E = 5.75 \cdot 10^{-5} \left(\left(G_f - G_{f,crit} \right)^2 \frac{d_h \rho_l}{\sigma \rho_v^2} \right)^{0.316} G_v \tag{3.5}$$

where G denotes mass flux, ρ density, σ surface tension and d_h is the hydraulic diameter of the channel. Indices v, l and f refer to the vapor phase, liquid phase and film, respectively. $G_{f,crit}$ is given by a separate correlation and denotes the onset of entrainment, i.e. the film flow rate below which no entrainment occurs.

The inventors of this correlation did not give any detailed motivation for its form, but it is written in terms of hydrodynamically relevant local parameters, such as the vapor mass flux and local film mass flux. (With some minor modifications equation 3.5 can be written in terms of the film wall flux, W_f/P, which is the physically relevant parameter if several films are present in the channel).

Okawa *et al.* (2003) presented an entrainment rate correlation based on dimensional reasoning and the hypothesis that the entrainment rate is primarily governed by the shear stress acting on the film (see also Okawa *et al.* (2002)). The authors gave the correlation in terms of the superficial velocities of film and vapor as:

$$E = k_e \rho_l \frac{f_i \rho_v J_v^2 \delta}{\sigma} \left(\frac{\rho_l}{\rho_v} \right)^n \tag{3.6}$$

$$\delta = \frac{1}{4} \sqrt{\frac{f_w \rho_l}{f_i \rho_v}} \frac{J_f}{J_v} d_h \tag{3.7}$$

where $k_e = 4.79 \cdot 10^{-4}$ m/s, $n = 0.111$ and f_i and f_w are the interfacial and wall friction factors respectively (definitions are not repeated here). Here J denotes the superficial velocity and δ models the film thickness.

Equation 3.6 can be rearranged into a form rather similar to equation 3.5 above. It then becomes:

$$E = k_e \frac{S f_i}{\sigma} \frac{d_h G_f}{4} \left(\frac{\rho_l}{\rho_v} \right)^n G_v \tag{3.8}$$

$$S = \sqrt{\frac{f_w \rho_l}{f_i \rho_v}} \tag{3.9}$$

where S is a model of the slip ratio.

In the same paper it was proposed that to this shear induced entrainment add a term for entrainment due to boiling, based on a correlation originally developed by Ueda *et al.* (1981) for falling liquid films. As was briefly discussed in Chapter 1, such heat flux induced phenomena are probably important in short channels with high heat flux, but when compared with the present data, the agreement was better without this term (see Paper 2).

A slightly different form of the correlation 3.6 was shown to be able to capture the influence of the axial power distribution on the dryout power in Okawa *et al.* (2004). This feature, and that the correlation is based on physical reasoning, made it interesting for comparison with data from the present project.

3.5. Models for the Boundary Condition

As mentioned above, the boundary condition at the onset of annular flow can be crucial for the success of the model if the channel is not very long. At the same time, this boundary condition is probably the most uncertain part of phenomenological dryout modeling, primarily because film flow measurements in this region are very difficult.

To close equation 3.1 it is necessary to specify the film flow rate at the beginning of annular flow as well as a model for where the transition to annular flow occurs. Unfortunately, correlations for deposition and entrainment are sometimes given without this informatin, which makes them difficult to apply in practice.

A common assumption is that deposition and entrainment are in equilibrium at the beginning of annular flow. This assumption was successfully used by Okawa *et al.* (2003), who used a correlation for the transition to annular flow and calculated film flow rate by setting the deposition and entrainment correlations equal at that point. Hewitt & Govan (1990) mention the assumption of 99% of the liquid to be entrained as drops at a quality of 0.1, but also that their results were insensitive to this assumption. Since this boundary condition would not reproduced the data presented here, the boundary condition given by Okawa *et al.* (2003) was used instead.

CHAPTER 4

Summary of Results

4.1. Critical Film Thickness

As was mentioned in Chapter 1 it is not fully clear whether the film flow rate goes continuously to zero when dryout is approached or if it suddenly breaks up at some positive critical film thickness. The measurements on the uniform power distribution are particularly useful to investigate this, by slightly extrapolating the results to the power where dryout was measured. (No measurements could be performed at dryout conditions for practical reasons). Such an investigation was presented in Paper 1 and it was concluded that for the investigated conditions the critical film thickness would, within the accuracy of the measurements, for practical purposes be negligible.

This conclusions is in agreement with measurements with similar conditions performed by Hewitt *et al.* (1965). Measurements in much shorter pipes (around 1 m) by e.g. Milashenko *et al.* (1989) and Ueda & Isayama (1981), however, have shown significant critical film thickness, indicating that the results of the present measurements are not valid for high enough heat fluxes.

4.2. Influence of the Power Distribution

In Chapter 1 the explanations by Bennett *et al.* (1966) of the influence of the power distribution were recapitulated. Their conclusion was that the effect is hydrodynamical and results in more entrained drops at the exit of the pipe if the power is shifted towards the outlet (in their case by introducing a cold patch close to the inlet).

The main purpose of the present project was to confirm these conclusions for realistic power distributions that can be found in a typical BWR. One difficulty was that the difference between the power distributions is rather small in tubes without spacers grids, see Figure 4.1. (It is much larger in complex geometries, such as rod bundles, that are always equipped with spacer grids). Thus, to see the effect the accuracy of the measurements must be quite high. Nevertheless, in Paper 3 it was demonstrated that the present measurements can resolve the difference between the inlet peaked and outlet peaked distributions and that the tendency in the entrained drop flow rate is consistent with the conclusions by Bennett *et al.* (1966). That is, there is more

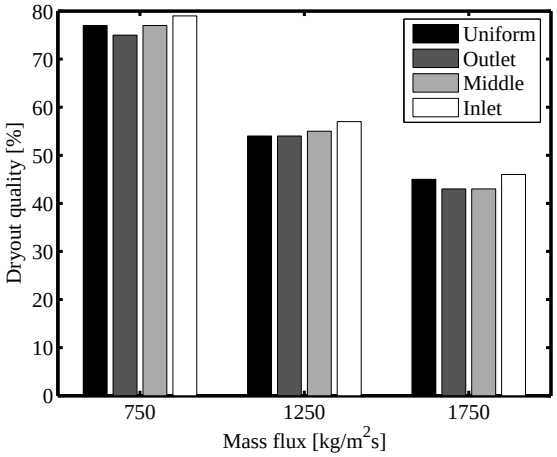

FIGURE 4.1. Dryout steam quality for the investigated conditions; four axial power distributions and three flow rates.

entrained drops and thus less film when the power distribution is outlet peaked. The results of the current measurements are illustrated in Figure 4.2.

As can also be seen in the figure it was difficult to conclude much for the middle peaked distribution, since the results were similar (within the accuracy of the measurements) to what was obtained for the inlet peaked profile.

4.3. Comparison with Models

Obviously, the measurements presented here should be compared with existing phenomenological models of annular flow and dryout. Two models, due to Hewitt & Govan (1990) and Okawa *et al.* (2003), were selected for this purpose. Both models use semi-empirical correlations, which have been tuned against measurements of film flow and dryout power, to describe the deposition and entrainment processes. One difference is that the second model contains a term that depends on the local heat flux and is supposed to model entrainment due to nucleate boiling within the liquid film (see Chapter 3.2).

In Paper 2 these two models were compared with the present measurements of the uniform and outlet peaked power distributions. It was concluded that both models were in excellent agreements with the measurements provided that the boiling entrainment term was removed from the second model. This result indicates that boiling entrainment is not a significant effect at the investigated conditions.

The comparison in Paper 2 was carried out by using one measurement point as boundary condition for the models, thus avoiding the problem of modeling the boundary condition. Paper 3 presented comparisons with the same two

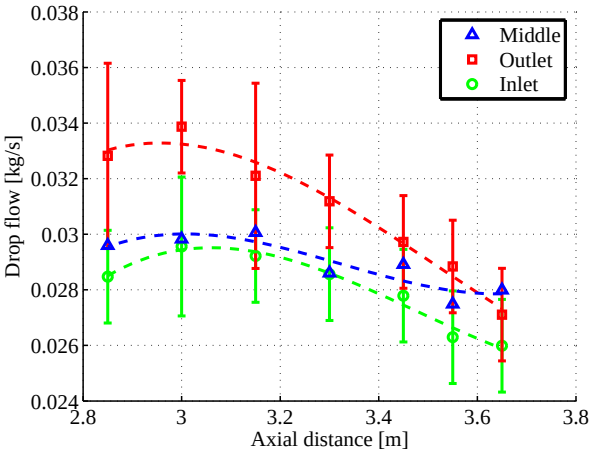

FIGURE 4.2. Drop flow versus axial distance for inlet-, middle- and outlet-peaked axial power distributions. Mean heat flux 0.74 MW/m^2, total mass flux 750 kg/m^{2}s, pressure 70 bar, inlet subcooling 10 K.

models but with the boundary condition proposed in the paper by Okawa *et al.* (2003). Again the agreement between models and measurements was excellent, but it is evident from Figure 4.3 that the largest difference between the models occur in the lower part of the channel where no measurements were available.

An intersesting observation, not included in any of the papers, is shown in Figures 4.4(a) and 4.4(b). As can be seen, the model by Okawa *et al.* (2003) correctly predicts the tendency of more entrained drops for the outlet peaked power distribution, but the model by Hewitt & Govan (1990) does not. One would then expect the latter model would also fail to predict the trend in dryout power, but this does not happen. The reason is that the erroneous trend seen in Figure 4.4(b) reverses when the power is increased and film flow approaches zero.

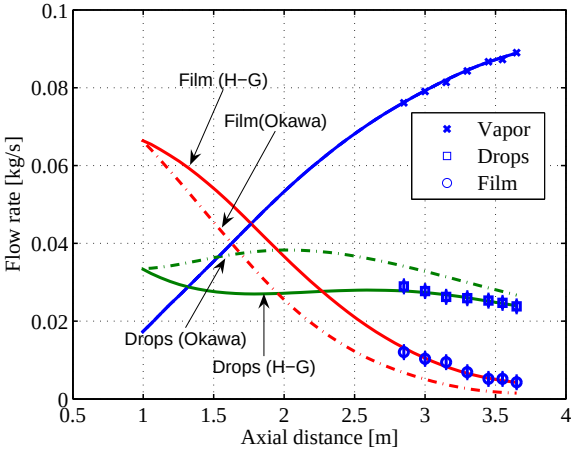

FIGURE 4.3. Comparison of measured flow rates with predictions by Hewitt & Govan (1990) and Okawa *et al.* (2003) models. Inlet-peaked axial power distribution, mean heat flux 0.86 MW/m^2, mass flux 1750 kg/m^{2}s, pressure 7 MPa and inlet subcooling 10 K.

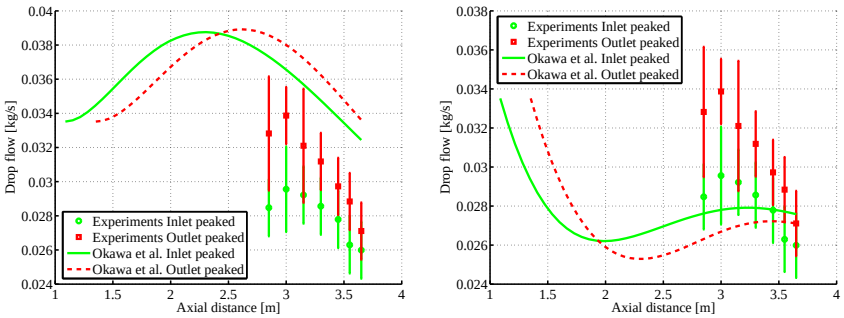

(a) Okawa *et al.* (2003) (b) Hewitt & Govan (1990)

FIGURE 4.4. Flow rate of entrained drops at mass flux 750 kg/m^{2}s and mean heat flux 0.74MW/m^2, according to experiments and two phenomenological models.

CHAPTER 5

Conclusions and Future Work

In this thesis measurements of the film flow rate in heated round tubes have been presented. The results show that the axial power distribution has an influence on the drop flow rate and thereby on the film flow rate and that this influence is consistent with the well known tendency in the dryout power. These results are consistent with other available data with simpler power distributions. The conclusion is that the hydrodynamical explanation of this effect is at least qualitatively correct also for power distributions and thermodynamic conditions typically found in a boiling water nuclear reactor.

It has also been shown that the film flow rate tends to zero (within the accuracy of the measurements) when the dryout power is approached. Hence no critical film model should be necessary for the heat flux and flow conditions considered here. Also this conclusion is consistent with earlier measurements at similar conditions.

Since the measurements presented here were carried out at several axial positions for each set of boundary conditions, they are well suited for comparison with phenomenological models of annular flow. The comparison that has been presented here shows that two selected phenomenological models well reproduce the experimental data. The largest discrepancy between the two models, however, occurred in the lower part of the channel where no measurements were available.

There are many ways this work could be extended and continued. If better accuracy could be achieved, a more detailed comparison of more power profiles would be possible. The simplest way to improve the accuracy is most probably to replace the flow meter in the extraction loop with a more accurate instrument. It might also be possible to improve the temperature measurements on the secondary side of the heat exchanger. Distorted extraction curves are more difficult to remedy, but having eliminated other error sources it might be possible to correct them for the effects of large disturbance waves.

The parameter range covered by the present project was very limited. It would be of interest to extend it, primarily to higher flow rates but also to vary the pressure and inlet temperature. The measurements would probably be more difficult at high flow rates, though (because of low steam quality and thus thick films a large amounts of entrained drops that can disturb the measurements).

It is also likely that capacity of the heat exchanger and flow meter must be extended to be able to handle higher flow rates.

Finally, it would be of interest to investigate the influence of spacer grids on the liquid film. Measurements of the dryout power show that spacer grids, depending on their design, can significantly increase the dryout power. Models for this effect exist, but there is not much detailed film flow data available for validation. With one moveable spacer close to the exit of the pipe, this effect could be investigated with the present equipment. It is also likely that one or more spacer grids in the pipe would increase the difference between the power distributions, thereby making a comparison between them easier.

Acknowledgements

First of all I would like to thank my supervisor Prof. Henryk Anglart for all support during the work and for interesting discussions, comments and criticism.

Stellan Hedberg cannot be thanked enough for making this project possible with his technical skills and knowledge, for constructing the equipment, repairing it when it broke down and for spending many hours in the lab with me during the measurements and error searching.

Thanks also to my co-supervisor Per Person for sharing his experience, the LABVIEW code for the main loop and for showing a lot of interest in the project.

The Swedish Center for Nuclear Technology (SKC) is gratefully acknowledged for their financial support and Westinghouse Electric Company for giving me the opportunity to do this. My reference group has contributed with valuable comments and generally showed interest in the project, which is appreciated.

Finally I would like to thank my colleagues and friends at KTH for creating a pleasant and creative working environment.

References

Bennett, A. & Thornton, I. 1961 Data on vertical flow of air-water mixtures in the annular and dispersed flow regions. part i: Preliminary study. *Trans. Inst. Chem. Engrs.* **39**, 101–112.

Bennett, A. W., Hewitt, G. F., Kearsey, H., Keeys, R. & Pulling, D. 1966 Studies of burnout in boiling heat transfer to water in round tubes with non-uniform heating. *Tech. Rep.* R5076. AERE.

de Bertodano, M. L. & Assad, A. 1998 Entrainment Rate of Droplets in the Ripple-Annular Regime for Small Vertical Ducts. *Nuclear Science and Engineering* **129**, 72–80.

Blomstrand, J., Behamin, D., Persson, P. & Hedberg, S. 2000 Loop studies simulating – in annular geometry – the influence of the axial power distribution and the number of spacers in 8x8 bwr assemblies. In *2nd Japanese-European Two-Phase Flow Group Meeting*.

Collier, J. G. & Hewitt, G. F. 1964 Film thickness measurement. *ASME paper 64–WA/HT–41* .

Groeneveld, D. 1975 The effect of short flux spikes on the dryout power. *Tech. Rep.* AECL–4927. Atomic Energy of Canada Ltd.

Hetsroni, G., ed. 1982 *Handbook of Multiphase Systems*. Hemisphere Publisher Corporation.

Hewitt, G. & Govan, A. 1990 Phenomenological modeling of non-equilibrium flows with phase change. *Int. J. Heat and Mass Transfer* **33** (2), 229–242.

Hewitt, G., Kearsey, H., Lacey, P. & Pulling, D. 1965 Burnout and film flow in the evaporation of water in tubes. *Tech. Rep.* R4864. AERE.

Hewitt, G. & Pulling, D. 1969 Liquid entrainment in adiabatic steam-water flow. *Tech. Rep.* R5374. AERE.

Hoyer, N. 1998 Calculation of dryout and post–dryout heat transfer for tube geometry. *International Journal of Multiphase Flow* **24** (2), 319–334.

Milashenko, V., Nigmatulin, B., Petukhov, V. & Trubkin, N. 1989 Burnout and distribution of liquid in evaporative channels of various lenghts. *International Journal of Multiphase Flow* **15** (3), 393–401.

Okawa, T., Kitahara, T., Yoshida, K., Matsumoto, T. & Kataoka, I. 2002 New entrainment rate correlation in annular two-phase flow applicable to wide

range of flow conditions. *International Journal of Heat and Mass Transfer* **45**, 87–98.

Okawa, T., Kotani, A., Kataoka, I. & Naito, M. 2003 Prediction of Critical Heat Flux in Annular Flow Using a Film Flow Model. *Journal of Nuclear Science and Technology* **40** (6), 388–396.

Okawa, T., Kotani, A., Kataoka, I. & Naito, M. 2004 Prediction of critical heat flux in annular regime in various vertical channels. *Nuclear Engineering and Design* **229**, 223–236.

Singh, K., Pierre, C., Crago, W. & Moeck, E. 1969 Liquid Film Flow-Rate in Two-Phase Flow of Steam and Water at 1000Lb/Sq.In.Abs. *AIChE Journal* **15** (1).

Sugawara, S. 1990 Droplet deposition and entrainment modeling based on the three-fluid model. *Nuclear Engineering and Design* **122** (67).

Ueda, T., Inoue, M. & Nagatome, N. 1981 Critical heat flux and droplet entrainment rate in boiling of falling liquid films. *International Journal of Heat and Mass Transfer* **24** (7), 1257–1266.

Ueda, T. & Isayama, Y. 1981 Critical heat flux and exit film flow rate in flow boiling system. *International Journal of Heat and Mass Transfer* **24** (7), 1267–1276.

Utsuno, H. & Kaminaga, F. 1998 Prediction of Liquid Film Dryout in Two-Phase Annular-Mist Flow in a Uniformly Heated Narrow Tube. Development of Analytical Method under BWR Conditions. *Journal of Nuclear Science and Technology* **35** (9), 643–653.

Würtz, J. 1978 An Experimental and Theoretical Investigation of Annular Steam-Water Flow in Tube and Annuli at 30 to 90 bar. *Tech. Rep.* 372. RisøNational Laboratory.

APPENDIX A

Power profiles

TABLE 1. Relative power for the four axial power distributions as function of the axial coordinate. The values were obtained by resistance measurements of the test-section. There is a spike in the inlet peaked profile due to a manufacturing fault.

z [m]	uni.	inl.	mid.	out
0.099	1.000	0.387	0.479	0.400
0.197	1.000	0.454	0.490	0.417
0.296	1.000	0.578	0.511	0.467
0.395	1.000	0.714	0.541	0.527
0.493	1.000	0.839	0.580	0.592
0.592	1.000	0.953	0.633	0.650
0.691	1.000	1.052	0.700	0.694
0.789	1.000	1.131	0.783	0.729
0.888	1.000	1.195	0.880	0.763
0.986	1.000	1.243	1.039	0.798
1.085	1.000	1.433	1.155	0.836
1.184	1.000	1.332	1.269	0.885
1.282	1.000	1.354	1.396	0.933
1.381	1.000	1.360	1.520	0.988
1.480	1.000	1.367	1.638	1.042
1.578	1.000	1.380	1.705	1.089
1.677	1.000	1.392	1.719	1.123
1.776	1.000	1.369	1.721	1.157
1.874	1.000	1.345	1.718	1.196
1.973	1.000	1.303	1.704	1.243
2.072	1.000	1.224	1.664	1.269
2.170	1.000	1.170	1.600	1.282
2.269	1.000	1.113	1.486	1.294
2.368	1.000	1.056	1.355	1.283
2.466	1.000	0.997	1.218	1.271
2.565	1.000	0.947	1.081	1.257
2.664	1.000	0.875	0.948	1.236
2.762	1.000	0.828	0.833	1.204
2.861	1.000	0.784	0.741	1.156
2.959	1.000	0.747	0.664	1.113
3.058	1.000	0.705	0.602	1.060
3.157	1.000	0.666	0.557	0.978
3.255	1.000	0.614	0.523	0.887
3.354	1.000	0.548	0.493	0.790
3.453	1.000	0.482	0.477	0.672
3.551	1.000	0.427	0.462	0.537
3.650	1.000	0.410	0.480	0.418

Part II

Papers

1

Paper 1

Measurements of the Liquid Film Flow Rate in High Pressure Annular Flow with Various Axial Power Distributions

By Carl Adamsson and Henryk Anglart

KTH Nuclear Reactor Technology, SE-106 91 Stockholm, Sweden

Published at *HEAT 2005*, Gdansk, Poland, June 26–30, 2005

Measurements at high pressure (70 bar) of the film flow rate in annular two-phase flow in a round heated tube are ongoing. The film is measured by extracting it through a porous wall section, condensing the sample and performing a heat balance calculation to find the liquid water content. This paper describes the measurement technique used and presents selected results. It is concluded that the critical film thickness is very small and that this is consistent with earlier measurements under similar conditions.
Keywords: dryout, film flow rate, film thickness, measurements

---

1. Introduction

In a boiling water nuclear reactor (BWR) one of the most important design limits is the dryout power and accurate predictions of this limit are thus needed. The traditional way to achieve this has been through empirical correlations based on full scale experiments. Such methods can be highly accurate but have some important drawbacks; the extensive full scale experiments that are needed are very expensive and the correlations obtained have no predictive capabilities outside the range of the experiments. This is particularly problematic when the effect of the spatial power distribution is concerned, since this is a parameter that is practically difficult to vary and that cannot be characterized by a single number. To capture such effects models funded in the underlying physical mechanisms are needed. These mechanisms are qualitatively known [1] but mechanistic dryout models cannot yet produce fully reliable quantitative results. Basically the amount of liquid film on the heated surface must be predicted, which requires accurate modeling of the delicate balance between deposition of drops to the film and entrainment and evaporation of the film. Not much information of these processes can be gained from measurements of the dryout power itself. Instead accurate measurements of the liquid film are needed.

2. Measurement Methods and Earlier Experiments

Several methods have been tried to measure the liquid film mass flow or liquid film thickness in annular flow. These are related, e.g. by the triangular relationship, see [2], but not equivalent. The film thickness has been measured with needle probes [3], [4] and with conductance probes [5]. Most basic mechanistic models of the dryout phenomenon are however based on fundamental mass- and energy equations where the mass flow rather than the film thickness occurs so the mass flow rate might be of more interest. This conclusion vastly reduces the number of available measurement techniques; measuring the film flow rate requires that the film is extracted from the flow. Such measurements have successfully been carried out by several groups by extracting the film through a porous wall section made from a sinter metal material. This has been done in low pressure air-water systems [6], low pressure steam-water system [7], [8], high pressure steam-water [9] and many others. It is also the method used in the present study. Bennet et al. [10] performed a series of very interesting measurements where the axial power profile had moveable cold patches. However there are, to the author's knowledge, no measurements available with various axial power profiles for several axial positions. Therefore this is the focus of the present program.

3. Experimental Setup

A sketch of the loop and film measurement system is shown in Figure 3. The test section consists of a 3.65 m long, 14.0 mm diameter stainless steel pipe directly heated by an electric current. The physical conditions in the loop were kept as close to normal operating conditions in a BWR as possible, i.e. 70 bar pressure, 10 K subcooling at the inlet and a mass flux in the test section in the interval 500-2000 kg/m^{2}s.

The porous section used for film flow measurements had an effective length of 3 cm and was installed just after the heated length. Through this section a sample of the flow is extracted, which will generally contain a mixture of liquid water and vapor. To determine the vapor content the sample is condensed in a carefully insulated heat exchanger and the temperatures and flow rates are measured on the primary as well as secondary side. The vapor content, x_{sample}, can then be calculated from the heat balance according to:

$$x_{sample} = \frac{W_2 \left(h_{2out} - h_{2in}\right) + W_1 \left(h_{out} - h_{sat}\right)}{W_1 h_{\mathrm{lg}}} \tag{1}$$

where W_1 and W_2 denote the mass flow rates at the primary and secondary side, respectively, and h_{out} the enthalpy on the outlet on the primary side. h_{2out}, h_{2in}, h_{sat} and h_{lg}, denote the enthalpies at the out- and inlet on the primary side, liquid saturation enthalpy and the latent heat of vaporization.

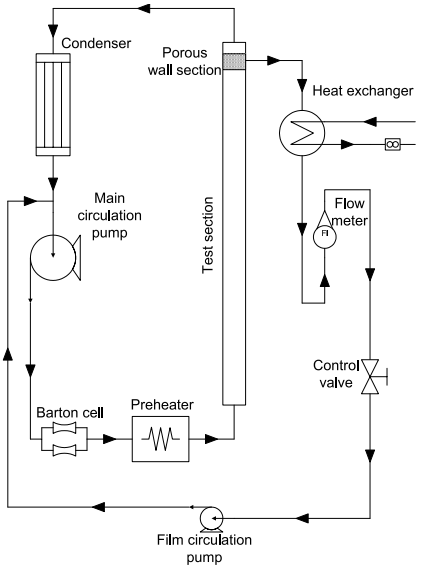

FIGURE 1. Working principle of the main loop and the film flow measurement system.

4. Procedure

During the test program four different axial power profiles will be investigated and the film flow rate measured at several axial locations, starting from the outlet and about 1.5 m upstream. Since the suction part is always mounted after the heated length its effective position can be changed only by disassembling the test section, cutting the pipe and mount it in the loop again. When the pipe has been cut and the measurements are to be started again it is important to exactly reproduce the conditions in the loop that existed before the cutting. The total power must decrease to keep the local (not the mean) wall heat flux constant. This was done by directly measuring the voltage over a part of the test section that was always upstream of the suction point.

When the power profile was uniform the boiling boundary was moved by adjusting the inlet temperature instead of cutting the pipe. It should be noted that it is the inlet temperature that should be changed and not the power since that would change the steam quality gradient in the loop.

To measure the film flow rate the sample flow extracted through the porous part was increased in steps from a low value (lower than the actual film flow) until steam was detected in the sample. Then it was concluded that the film flow rate was reached. The vapor fraction in the sample was continuously calculated by the heat balance over the heat exchanger (1) and the film flow

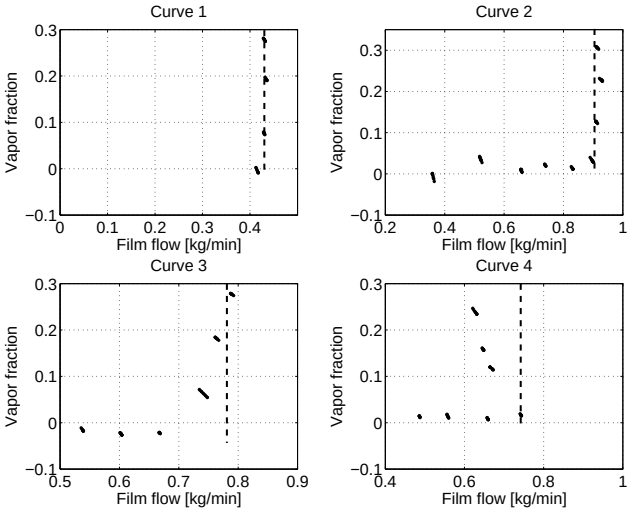

FIGURE 2. Examples of suction curves from the experiments and their interpretation.

was calculated as, $W_f = (1 - x_{sample})\, W_1$. As the sample flow was increased x_{sample} was plotted versus W_f. Ideally this should result in a curve with a horizontal part of zero vapor fraction for low sample flows and a vertical part with constant liquid flow when the sample flow exceeds the film flow rate in the test section. Examples of suction curves that were obtained in the experiments are shown in Figure 4. As can be seen the curves do not always have this ideal L-shape. This has several reasons. The first curve is missing the horizontal part simply because the flow rate was too low to be accurately measured, but the vertical part still makes it possible to estimate the film flow. The second curve is close to the ideal curve. The horizontal part shows a vapor fraction slightly different from zero but this error was never larger than 10%. The third curve bends towards higher film flow when the sample flow is increased, probably because drops from the gas core are captured together with the film. This usually occurred for thick films at low steam quality. The fourth curve bends towards lower film flow with increasing sample flow. This must probably be explained by measurement errors. For such curves it was decided to let the point that indicated the largest film flow rate represent the real film flow.

5. Results

The measurements are currently ongoing and the complete results will be published elsewhere. Included here are the results for the uniform power profile in Figure 5. In the figure is also indicated the measured dryout steam quality. As

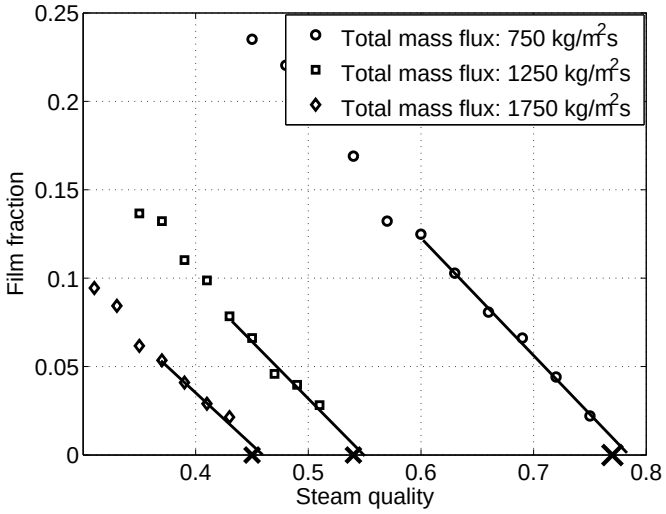

FIGURE 3. Results from film flow measurements with uniform power profile at 70 bar.

can be seen the film flow curves extrapolate almost to zero at the dryout point. This is consistent with the results in [7].

6. Errors and Sensitivity

The method of extracting the film through a porous wall section is discussed in [9] and it is recommended that the porous part should have a length of 1 in. This is very close to what is used in the present study. One should also consider the possibility that droplets deposit on the wall after the heated length but before the extraction point and that vapor may condense before the heat exchanger. These effects should however be very small since the distances involved are small and the pipes well insulated.

The sensitivity of the results due to inaccuracies in the measurements of flow rates and temperatures can be found be differentiating equation (2), which gives:

$$\frac{\partial W_f}{\partial W_1} = 1 + \left(\frac{h_{sat} - h_{out}}{h_{\mathrm{lg}}} \right) \approx 2 \tag{2}$$

$$\frac{W_2}{W_1}\frac{\partial W_f}{\partial W_2} = -\left(\frac{h_{sat} - h_{out}}{h_{\mathrm{lg}}} + x_{sample} \right) \approx -1 \tag{3}$$

$$\frac{1}{W_1}\frac{\partial W_f}{\partial T_{out}} = \frac{C_p}{h_{\mathrm{lg}}} \approx -0.003\frac{1}{K} \tag{4}$$

$$\frac{1}{W_1}\frac{\partial W_f}{\partial T_{2out}} = -\frac{1}{W_1}\frac{\partial W_f}{\partial T_{2in}} = \frac{W_2}{W_1}\frac{C_p}{h_{\mathrm{lg}}} \approx -0.06\frac{1}{K} \tag{5}$$

The numerical values were found by substituting typical values obtained from the measurements for the different parameters. As can be seen the sensitivity to errors in the temperature measurements on the primary side is very small. W_2 was repeatedly confirmed during the measurements and found to be accurate within 2%. T_{2in} and T_{2out} were measured by several thermocouples showing the same temperature within ± 0.5 K, which can be estimated from (5) to give an error of 6%. The flow meter on the primary side showed a standard deviation of 4% when it was calibrated. According to (2) this gives an error of 8%. These results are consistent with the observation that the calculated vapor content does not deviate more than 10% from zero when single phase flow is maintained in the film loop. From this it can be concluded that the accuracy of the measurements should be within 10–15%.

Another observation worth mentioning is the repeatability of the results. Each of the three curves shown in Figure 5 was assembled during two days and the loop was closed and cooled down in between. Because of this a slight zigzag pattern can be seen in the curve for 1250 kg/m^{2}s. This can be taken as a measure of the repeatability which must be considered as satisfactory.

7. Conclusions

Measurements of the film flow rate in annular flow in round tube geometry with various axial power distributions are ongoing. The results obtained so far are consistent with previous measurements in that the liquid film flow approaches zero at the dryout point. The accuracy of the measurements has been estimated to be within 10–15% in the film mass flow rate.

References

1. Hetsroni, G., 1982, *Handbook of multiphase systems.* ISBN 0-07-028460-1
2. Hewitt, G.F. and Whalley, P.B.,1989, *Vertical annular two-phase flow*, *in Multiphase Science and Technology*, Vol. 4, ISBN 0-89116-649-1
3. Neal, L. G. and Bankoff, S. G. 1963 A high resolution resistivity probe for determination of local void properties in gas-liquid flow. AIChE Jl **9**, 490.
4. Würtz J., 1978, *An experimental and theoretical investigation of annular steam-water flow in tubes and annuli at 30 and 90 bar*, Risö Report No. 372
5. Collier, J. G. and Hewitt, G. F. 1964. *Film thickness measurement.* ASME Paper 64-WA/HT-41.
6. Whalley P.B, Hewitt G.F, Hutchinson P. (1973). Experimental wave and entrainment measurements in vertical annular two-phase flow. AERE R7521
7. Hewitt G.F, Kearsey H.A., Lacey, P.M.C. and Pulling, D.J., 1965. *Burnout and film flow in the evaporation of water in tubes.* AERE R4864
8. Hewitt G.F and Pulling D.J.(1969). Liquid entrainment in adiabatic steam-water flow. AERE-R5374

9. Singh, K., Pierre, C.C. St., Crago, W.A., Moeck, E.O., 1969, *Liquid Film Flow-Rate in Two-Phase Flow of Steam and Water at 1000 Lb./Sq. In. Abs.* AIChE Journal **15**(1)
10. Bennet A. W., Hewitt, G. F., Kearsey H.A. , Keeys R.K.F. and Pulling D.J. 1966. *Studies of burnout in boiling heat transfer to water in round tubes with non-uniform heating.* AERE-R5076

2

Paper 2

Eperimental Investigation of the Liquid Film for Annular Flow in a Tube with Various Axial Power Distributions

By Carl Adamsson and Henryk Anglart

KTH Nuclear Reactor Technology, SE-106 91 Stockholm, Sweden

Published at *NURETH11*, Avignon, France, October 2–6, 2005

New measurements of the liquid film flow rate in annular water/steam flow in a heated tube at high pressure are presented. The axial power profile has been varied and the measurements have been carried out at several axial locations. The data are compared with two mechanistic dryout models and good agreement can be seen, but the inclusion of a term for boiling entrainment causes one of the models to deviate from the measurements.

---

1. Introduction

The phenomenon of critical heat flux (CHF) plays an important role in many boiling systems, such as water cooled nuclear reactors, since it sets an upper limit to the power production. Essentially there are two different mechanisms that can result in the sharp temperature rise that defines CHF. The first is usually called departure from nucleate boiling (DNB) and occurs when a thin vapor film is created near the heated surface thus isolating the wall from the flowing liquid. The second type, usually called dryout, occurs in the annular flow regime when the thin water film on the wall completely evaporates and leaves the wall in direct contact with the vapor core. This paper deals only with CHF of dryout type. The modeling of dryout has classically been based on empirical correlations since no accurate theory has been available. As nuclear reactor fuel has become more optimized the need for accurate predictions of the dryout power has grown and the traditional correlations do not satisfy the new demands. In particular the spatial power distribution is hard to catch with a correlation since it cannot be characterized by a single number. This situation has created a great interest in mechanistic models of the dryout phenomenon that can directly calculate the amount of liquid film. To create and verify such models quite specific experimental data are needed. To create an empirical correlation it is enough to have detailed measurements of the dryout power for a wide range of parameters and plenty of such data are available, but for a mechanistic model it is preferable to have direct measurements of the liquid

film in addition to the dryout power. In this paper such measurements are presented with focus on the influence of the axial power distribution.

2. Background

2.1. *Models*

A common way to model the liquid film mass balance is by the equation:

$$\frac{1}{\Pi}\frac{dW_f}{dz} = D - E - \frac{q}{h_{\mathrm{lg}}}. \tag{1}$$

Here W_f is the mass flow rate of liquid film and Π is the wall perimeter. D, E, q and h_{lg} denote the deposition- and entrainment rates of liquid film, the local wall heat flux and the latent heat of vaporization respectively. This equation will give the liquid film flow as a function of the axial position, provided that the expressions for the deposition and entrainment rates are known as well as appropriate boundary conditions. The mechanisms of deposition and entrainment from the film are very complex processes and the most realistic approach is probably to describe them with correlations of experimental data. In order to capture complicated effects, such as the influence of the axial power profile, it is however important that such correlations behave in a physically correct manner and extrapolate well. Many attempts to such correlations have been presented. Some of them are reviewed here; others can be found in the literature.

Hewitt and Govan (1990) presented the following pair of correlations for the deposition- and entrainment rates:

$$E = 5.75 \cdot 10^{-5} \left(\left(G_f - G_{crit}\right)^2 \frac{d_h \rho_l}{\sigma \rho_g^2} \right)^{0.316} G_g \text{ if } G_f > G_{crit} \tag{2}$$

where

$$\frac{G_{crit} d_h}{\mu_l} = \mathrm{Re}_{crit} = \exp\left(5.8504 + 0.4249 \frac{\mu_g}{\mu_l}\sqrt{\frac{\rho_g}{\rho_l}}\right), \tag{3}$$

and

$$D = k_d C, \tag{4}$$

where

$$C = \frac{W_d}{\frac{W_d}{\rho_l} + \frac{W_g}{\rho_g}}, \tag{5}$$

and

$$k_d = \begin{cases} 0.18\sqrt{\frac{\sigma}{\rho_g d_h}} \text{ if } \left(\frac{C}{\rho_g}\right) < 0.3 \\ 0.083\sqrt{\frac{\sigma}{\rho_g d_h}} \left(\frac{C}{\rho_g}\right)^{-0.65} \text{ if } \left(\frac{C}{\rho_g}\right) > 0.3 \end{cases}. \tag{6}$$

This model has been shown to predict both the dryout power and the liquid film flow rate when compared to measurements (Hewitt and Govan, 1990, Anglart and Adamsson, 2003). Of particular interest is the ability to predict the film

flow in the series of experiments performed by Bennet *et al.* (1966) where power profiles with a moveable cold patch were used.

A similar model has been presented by Okawa *et al.* (2003). This model has shown good ability to predict the dryout power in round tubes for a wide range of conditions (Okawa *et al.* 2002, Okawa *et al.* 2003, Okawa *et al.* 2004). The correlation for shear-induced entrainment rate is:

$$E = k_e \rho_l \frac{f_i \rho_g J_g^2 \delta}{\sigma} \left(\frac{\rho_l}{\rho_g} \right)^n , \tag{7}$$

where $k_e = 4.79 \cdot 10^{-4}$m/s and $n = 0.111$ and f_i and δ denote the interfacial friction factor and the film thickness respectively. This seems to be more physically motivated than the Govan correlation presented above.

Common to both these models are that the local wall heat flux does not enter into the correlations for deposition and entrainment. It should be noted that Okawa adds a boiling entrainment, which depends on the local heat flux, to the shear-induced entrainment given above.

On the other hand a very different model was presented by Milashenko *et al.* (1989). They claimed that the deposition of droplets is negligible when a wall heat flux is present and modeled the entrainment rate according to:

$$E = \frac{W_f}{(\pi d_h)^2} 1.75 \left[q \cdot 10^{-6} \left(\frac{\rho_g}{\rho_l} \right) \right]^{1.3} . \tag{8}$$

(This is a dimensional correlation where q must be given in the units of W/m^2). Clearly this model depends strongly on the local heat flux. It should be noted that this correlation was based on experiments in tubes that were much shorter than the tubes used in the present experiments and the fuel assemblies in most nuclear reactors.

Another important difference between the models above is the condition for dryout. Hewitt and Govan assume that the film flow rate will go smoothly to zero as the dryout point is approached but Milashenko *et al.* argue that the film flow rate at dryout is generally greater than zero, the so called critical film flow. Okawa *et al.* use a small value for the critical film flow that has almost no impact on the dryout power.

There seems to be little agreement on which approach of modeling is correct and many advanced dryout codes use combinations and modifications of the ideas mentioned above (Hoyer 1997, Sugawara, 1990).

The best way to validate these models should be to compare them with direct measurements of the liquid film flow, since data on the dryout power only do not generally contain enough information. Measurements of the film flow rate are available but usually the axial power profile has not been varied.

2.2. *Previous Experiments*

A series of very interesting measurements of the film flow rate where carried out by Bennet *et al.* (1966). They used a uniform power profile with a moveable cold patch. Both the dryout power and the axial film flow distribution were measured for various placements of the cold patch. This work offers a good qualitative explanation of the mechanisms by which the power profile influences the dryout power. The film flow measurements were performed only at low (atmospheric) pressure and cold patch power profiles even though the dryout power was measured also at higher pressure and for other profiles. The aim of the present experiments is to extend these measurements to higher pressure (reactor conditions) and more realistic power profiles.

Other interesting measurements of liquid film flow were performed by Moeck (1970) for developing films and by Mannov (1973) for high pressure in annular geometry.

3. Description of the Experiments

The experiments were performed in the high pressure dryout loop at Royal Institute of Technology, Sweden. Tube geometry was used in order to have only one film to measure. The conditions in the loop were kept as close to realistic BWR conditions as possible; the heated tube length was 3.65 m, tube diameter 13.9 mm, pressure 70 bar and mass flow rates from 500 to 1750 kg/m^{2}s were used. The tube, made from stainless steel, was heated directly by an electric current. The axial power profile was imposed by letting the outer tube diameter, and thereby the wall thickness, vary along the tube.

The film measurements were carried out by a procedure very similar to the one used by Bennet *et al.* (1966) and others. A 3.0 cm porous tube section, made of sinter metal material, was mounted directly after the heated length. A sample flow was sucked through the porous part, condensed completely in a heat exchanger, and then returned into the main loop before the beginning of the heated length. Since it is inevitable that some steam will be sucked out together with the liquid film it is necessary to measure the steam content in the sample. This was done by carefully measuring the temperatures on the inlet and outlet of the heat exchanger on the primary as well as on the secondary side. The steam content, x_{sample}, can then be found by a heat balance calculation according to:

$$x_{sample} = \frac{W_2 \left(h_{2out} - h_{2in}\right) + W_1 \left(h_{out} - h_{sat}\right)}{W_1 h_{\mathrm{lg}}}, \tag{9}$$

where W_2 and W_1 denote the mass flow rates at the secondary and primary side of the heat exchanger respectively. h_{2out}, h_{2in} and h_{out} are the specific enthalpies at the in- and outlets of the secondary and primary sides. The steam content was calculated continuously during the experiments and the sample flow rate was slowly increased in steps from a very low value (lower than the film

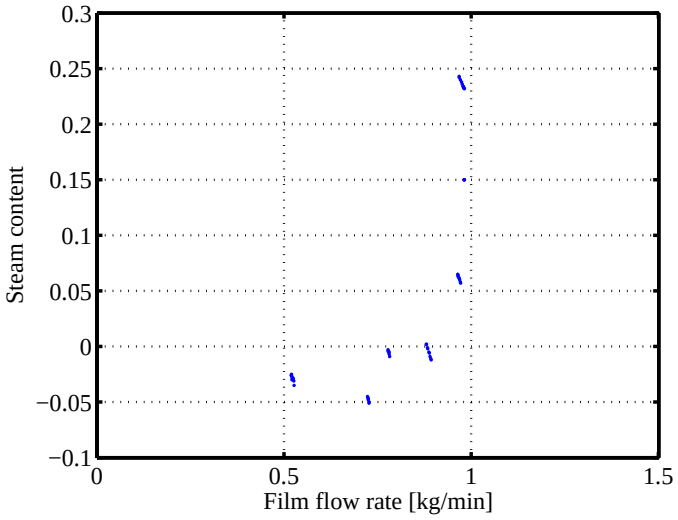

FIGURE 1. Example of a suction curve. In this case the film flow is approximately 1.0 kg/min.

flow rate) until the steam content was seen to sharply increase. At this point it was concluded that film flow rate hade been reached. If x_{sample} is plotted against $W_1\,(1 - x_{sample})$ and L-shaped curve will appear where the film flow can easily be read of. An example of such a curve is shown in Figure 3.

Since the porous wall section is always located directly after the heated length it is necessary to dismount the test section, cut the tube and reassemble it again to change the axial position of the filter. After the tube has been cut the total power must of course be decreased so that the local heat flux is preserved in order to achieve the same conditions in the loop. An exception to this is when the power profile is uniform. Then cutting the tube is equivalent to increasing the inlet subcooling, thereby moving the boiling boundary and decreasing the boiling length. This is naturally a much faster procedure. It should be noted that the boiling boundary should be moved by increasing the subcooling and *not* by decreasing the power. This is because the latter procedure would change the heat flux and thereby the steam quality gradient along the tube.

The experimental matrix is given in Table 1. It was decided to keep the pressure and inlet subcooling constant at 70 bar and 10 C respectively, since the experiments are very time consuming. For each set of conditions in the loop the film flow was measured at several axial positions distributed from the outlet and approximately 1 m upstream. Further upstream it was hard to get any

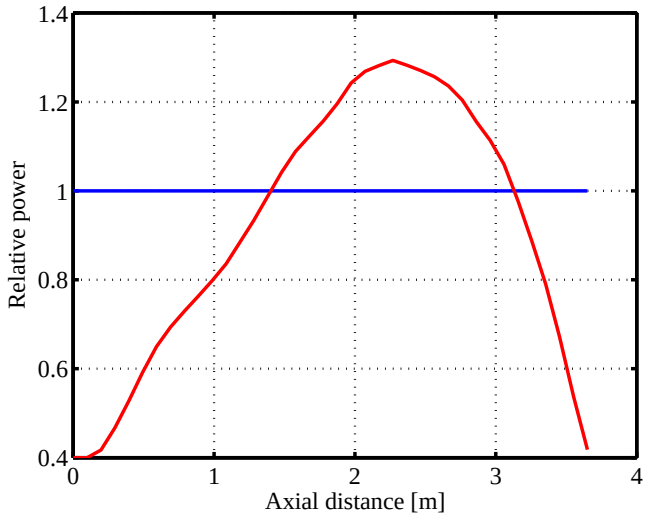

FIGURE 2. The top peaked and uniform power profiles used in the experiments.

accurate measurements, primarily due to the thick and not sharply defined film and difficulties to maintain stable conditions in the loop at low steam content. Figure 3 shows the axial power profiles used in the eperiments.

TABLE 1. Experimental matrix.

Flow rate [kg/m^{2}s]	Outlet quality	Power profile	Outlet quality at dryout
750	75%	Uniform	77%
1250	51%	Uniform	54%
1750	43%	Uniform	45%
750	72%	Top peaked	75%
750	65%	Top peaked	75%
1250	50%	Top peaked	54%
1250	45%	Top peaked	54%
1750	40%	Top peaked	43%
1750	36%	Top peaked	43%

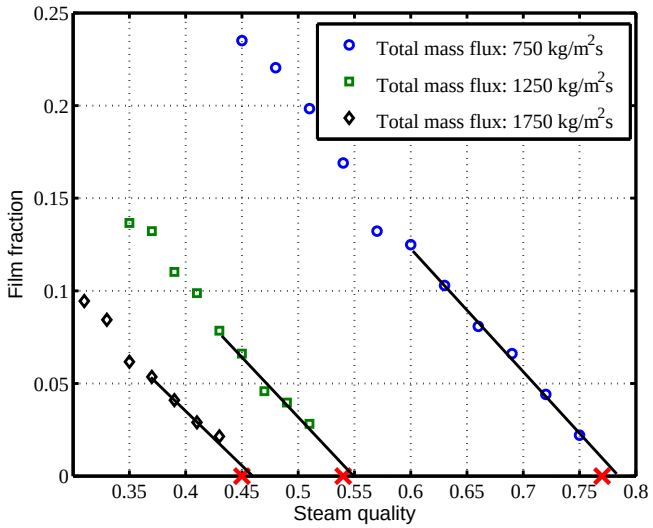

FIGURE 3. Film fraction against steam quality for the measurements with uniform power profile with different mass velocities. The steam quality where dryout occurred is indicated in each case.

4. Results

Figure 4 shows the measured film fraction against local steam quality when conditions in the loop were close to dryout. The quality at which dryout occurred is also indicated in the figure. The film curves extrapolate almost to the point of dryout. The small deviation could be interpreted as a very small critical film flow. One should, however, be careful when interpreting the data, since systematic errors can be present in the measurements; see the paragraph about error analysis below. These results can be compared to the very similar results reported by Hewitt et al (1965).

Figures 4 through 6 show the flow rates of vapor, drops and film versus axial length for the uniform power profile. In the figures are also curves showing simulated results according to equation (1) with the Govan correlation (2) and with the Okawa correlation (7). The integration of (1) was started from the axial location of the first data points, thus circumventing the problem to find appropriate boundary conditions at the beginning of annular flow. As can be seen in the figures the agreement of the Govan correlation with measured data is excellent. The correlation by Okawa seems to predict too much entrainment

for thick films. This, however, stems solely from the inclusion of the boiling entrainment term. If this term is omitted the results are almost indistinguishable from the predictions of the Govan correlation. This close agreement between the two correlations is true for the part of the tube where the measurements were made, but further upstream where the steam quality is lower and the film much thicker the two models deviate significantly. A conclusion from these observations is that improvements of the models should, surprisingly, be concentrated on thick film region and the boundary condition at the beginning of annular flow. Unfortunately the experimental equipment used for the present study was not able to work under such conditions.

Figures 7 through 9 show the results of film measurements with the top peaked power profile. The left plot in each figure shows the results of the measurements performed close to the dryout power and the right plots show the results at reduced power; compare Table 1.Few data points are currently available, but one can see that the drop flow rate is slowly decreasing towards to the outlet in good agreement with the models in a way similar to the results for the uniform power profile. By comparing the left and right plot in each figure it can also be seen that the drop flow rate changes only slightly when the power is reduced from the dryout power.

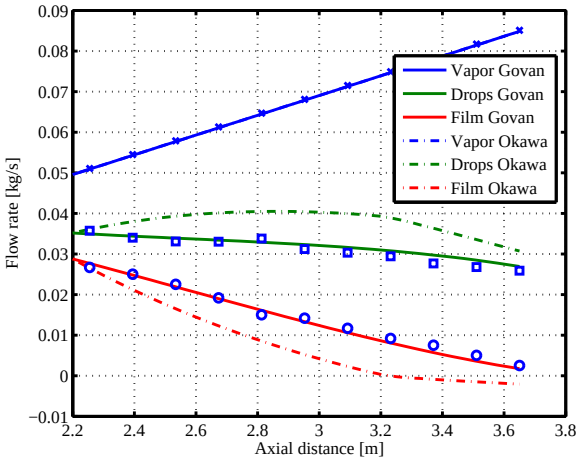

FIGURE 4. Measurements and simulations at 750 kg/m^{2}s and uniform power profile.

5. Error Analysis

There are several sources of errors that can influence the measurements. Noise will be introduced by difficulties to keep the working conditions of the main loop

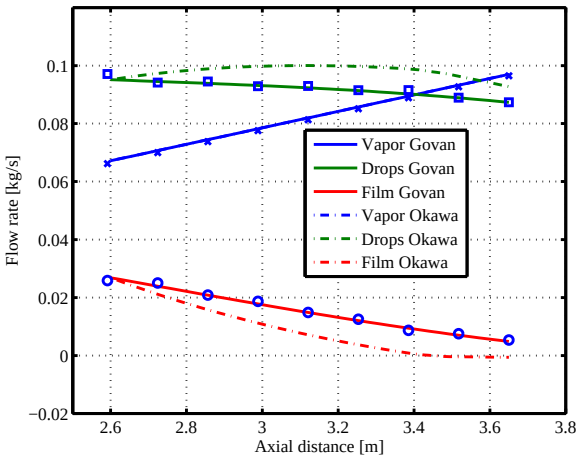

FIGURE 5. Measurements and simulations at 1250 kg/m^{2}s and uniform power profile.

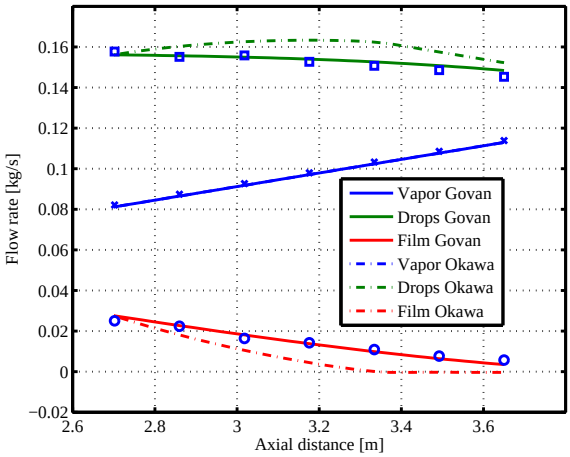

FIGURE 6. Measurements and simulations at 1750 kg/m^{2}s and uniform power profile.

stable during the measurements and by limited accuracy of the instruments for flow- and temperature registration. Nevertheless the reproducibility is quite good as can be seen from the curves in the last paragraph; the points on one such curve were usually collected during two days and the loop was closed and

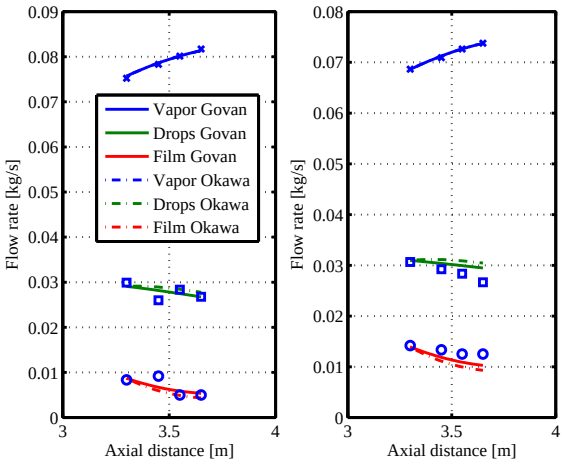

FIGURE 7. Measurements and simulations at 750 kg/m^{2}s and top peaked power profile. In the left plot the power is close to the dryout power, in the right plot the power is reduced.

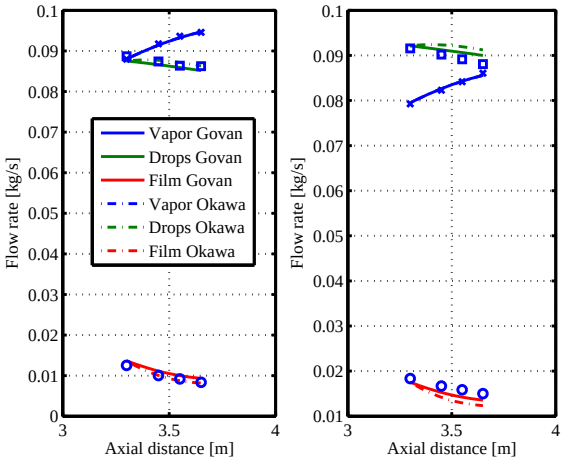

FIGURE 8. Measurements and simulations at 1250 kg/m^{2}s and top peaked power profile. In the left plot the power is close to the dryout power, in the right plot the power is reduced.

cooled down in between. Because of this a slight zigzag pattern can be seen in the measurements in Figure 4 (every second point was collected the first day

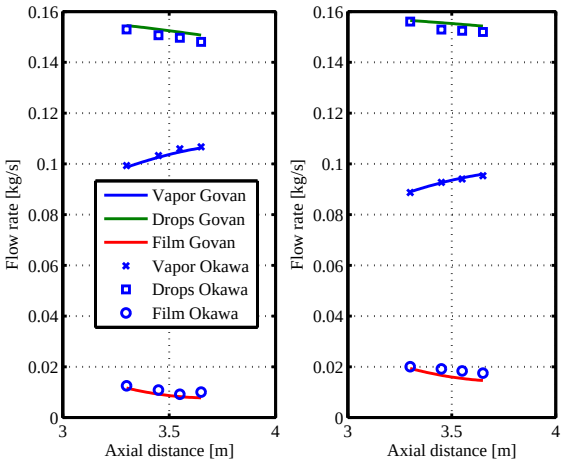

FIGURE 9. Measurements and simulations at 1750 kg/m^{2}s and top peaked power profile. In the left plot the power is close to the dryout power, in the right plot the power is reduced.

and the ones in between the second day). This can be taken as a measure of the random error in the measurements. As can be seen in Figure 4 this uncertainty seems to be larger for thicker films and lower steam qualities in the loop.

The results can also be influenced by some systematic biases. Small heat losses both in the test section itself and in the heat exchanger in the film measurement system are unavoidable. This may give a slight bias to the measurements that offers an alternative explanation to the apparent critical film flow in Figure 4. Another error source that could bias the measurements is redeposition of drops to the wall on the way from the heated test section to the filter part. This however, should be very small considering the short distance (4.0 cm) and the very low deposition rates that can be seen in Figures 4 through 6.

To quantify the sensitivity of the results to errors in different parameters it is of interest to analyze the formula used to calculate the film flow rate:

$$W_f = W_1 \left(1 - x_{sample}\right), \tag{10}$$

where x_{sample} is calculated by equation (9). Differentiating this gives:

$$\frac{\partial W_f}{\partial W_1} = 1 + \left(\frac{h_{sat} - h_{out}}{h_{\mathrm{lg}}}\right) \approx 2, \tag{11}$$

$$\frac{W_2}{W_1}\frac{\partial W_f}{\partial W_2} = -\left(\frac{h_{sat} - h_{out}}{h_{\mathrm{lg}}} + x_{sample}\right) \approx -1, \tag{12}$$

$$\frac{1}{W_1}\frac{\partial W_f}{\partial T_{out}} = \frac{C_p}{h_{\mathrm{lg}}} \approx -0.003\frac{1}{K}, \tag{13}$$

$$\frac{1}{W_1}\frac{\partial W_f}{\partial T_{2out}} = -\frac{1}{W_1}\frac{\partial W_f}{\partial T_{2in}} = \frac{W_2}{W_1}\frac{C_p}{h_{\mathrm{lg}}} \approx -0.06\frac{1}{K}. \tag{14}$$

The numerical values have been obtained by using typical values for the flow rates and enthalpies from the experiments. As can be seen from these equations the sensitivity to errors in the temperature on the primary side is very low. The calibration of the flowmeter on the secondary (cooling) side showed that it is accurate within 2%. Errors in the temperature on the secondary side and in the primary (sample) flow rate will have a greater influence, which must be considered. The temperatures on the secondary side were measured by several thermocouples in different positions, which all showed the same temperature to within ±0.5 K. From (14) this can be estimated to give rise to an error of 6%. When the flow meter on the primary side was calibrated, a standard deviation of 4% was obtained (probably more from difficulties to keep the flow rate stable than from the flow meter itself). According to (11) this can be expected to give an error of 8%. These observations are consistent with the single-phase heat balance being sometimes 5–10% off, as can be seen from the horizontal part of the curve in Figure 3. However, an equally large error source is probably the interpretation of the suction curves, since they are not always as well defined as in Figure 3. Thus, it can be concluded that the accuracy of the measurements should be within 10–15% with a possible small bias due to heat loss effects.

6. Conclusions

Direct measurements of the liquid film flow rate at several axial locations show that the correlations by Hewitt and Govan (1990) and by Okawa *et al.* (2003) give excellent fit to data when the film flow rate is low, i.e. close to dryout conditions. It is also shown that the inclusion of a model for boiling entrainment in the model by Okawa *et al.* seems to overpredict the entrainment rate. The measurements of the film flow rate when the power was very close to the dryout power revealed very thin films and a slight extrapolation of the measurements indicates that if there is a so called critical film flow (or critical film thickness) it is small for the conditions examined here.

The comparison of predictions with current experimental data indicates that models perform quite well for the two axial power profiles investigated so far. Naturally, more data are needed to draw fully valid conclusions, and this will be the subject of continued investigations.

7. Nomenclature

Latin letters:

C - effective drop density, kg m^{-3}

C_p- constant pressure heat capacity, J kg^{-1} K^{-1}

D - drop deposition rate, kg m^{-2} s^{-1}

d_h- hydraulic diameter, m

E - drop entrainment rate, kg m^{-2} s^{-1}

f_i- interfacial friction factor, dimensionless

G - mass flux, kg m^{-2} s^{-1}

J - superficial velocity, m s^{-1}

h_{lg}- latent heat of water, J kg^{-1}

h_{sat}- enthalpy of saturated liquid water, J kg^{-1}

k_d- deposition coefficient, m s^{-1}

k_e- entrainment coefficient, m s^{-1}

q - heat flux, W m^{-2}

Re - Reynolds number, dimensionless

T - temperature, K

W - mass flow rate, kg s^{-1}

x - steam quality, dimensionless

Greek letters:

δ – film thickness, m

μ – viscosity, Pa s

ρ – density, kg m^{-3}

σ – surface tension, N m^{-1}

Subscripts:

f - film

g - gas phase

in - inlet

out - outlet

l - liquid phase

1 - primary side of heat exchanger

2 - secondary side of heat exchanger

Acknowledgements

This research was sponsored by the Swedish Center for Nuclear Technology.

The authors also would like to thank Stellan Hedberg for all the technical support that has made this project possible.

References and Citations

Anglart, H. and Adamsson, C. 2003. *Modeling of dryout in channels with various spatial power distributions.* The 10^{th} International Topical Meeting on Nuclear Reactor Thermal Hydraulics (NURETH-10)

Bennet A. W., Hewitt, G. F., Kearsey H.A. , Keeys R.K.F. and Pulling D.J. 1966. *Studies of burnout in boiling heat transfer to water in round tubes with non-uniform heating.* AERE-R5076

Hewitt, G.F, Kearsey H.A., Lacey, P.M.C. and Pulling, D.J., 1965. *Burnout and film flow in the evaporation of water in tubes.* AERE R4864

Hewitt, G.F. and Govan A.H., 1990. *Phenomenological modeling of non-equilibrium flows with phase change.* International Journal of Heat and Mass Transfer, **33(2)**, 229-242.

Hoyer, N., 1998. *Calculation of dryout and post-dryout heat transfer for tube geometry.* International Journal of Multiphase Flow, **24(2)**, 319-334.

Okawa, T., Kotani, A., Kataoka, I. and Naitoh, M. 2004. *Prediction of critical heat flux in annular regime in various vertical channels.* Nuclear Engineering and Design, **229**, 223-236

Okawa, T., Kotani, A., Kataoka, I. and Naitoh, M. 2003. *Prediction of critical heat flux in annular regime in various vertical channels.* Journal of Nuclear Science and Technology, **40(6)**, 388-396

Okawa, T., Kitahara T., Yoshida, K., Matsumoto T. and Kataoka, I. 2002 *New entrainment rate correlation in annular two-phase flow applicable to wide range of flow conditions.* International Journal of Heat and Mass Transfer, **45**, 87-98.

Mannov, G., 1973. *Film flow measurements in concentric annulus 3500x27.2x17 mm with heated and unheated rod.* SDS-65, Danish Atomic Energy Commission, Risö, Denmark.

Milashenko, V.I., Nigmatulin, B.I., Petukhov, V.V and Trubkin, N.I., 1989. *Burnout and distribution of liquid in evaporative channels of various lengths.* International journal of multiphase flow, **15(3)**, 393-401.

Moeck, E.O. 1970. *Annular-dispersed two-phase flow and critical heat flux.* AECL-3656.

Sugawara, S., 1990. *Droplet deposition and entrainment modeling based on the three-fluid model.* Nuclear engineering and Design, **122**, 67-84

Paper 3

3

Film Flow Measurements for High Pressure Diabatic Annular Flow in Tubes with Various Axial Power Distributions

By Carl Adamsson and Henryk Anglart

KTH Nuclear Reactor Technology, SE-106 91 Stockholm, Sweden

Submittid to *Nuclear Engineering and Design*

Measurements of film flow rates in diabatic annular flow in tubes with various axial power distributions were carried out in the high-pressure two-phase flow loop at the Royal Institute of Technology (KTH), Sweden. The measurements were performed at conditions typical for boiling water reactors, i.e. 7 MPa pressure and total mass flux in a range from 750 to 1750 kg/m^{2}s. Four different axial power distributions were used and the film mass flow was measured at 7 axial locations for each set of boundary conditions. The results show that the outlet peaked distribution gives less film than the inlet peaked one. This result is consistent with well known trends from measurements of dryout power. The measurements also show that the film flow at the onset of dryout is very small at investigated conditions in agreement with earlier studies. Finally it is shown that the present data is well predicted by two selected phenomenological models of annular flow.

---

1. Introduction

In various boiling systems, such as water cooled nuclear reactors, the critical heat flux (CHF) phenomenon is one of the main design constraints, since it sets an upper limit to the possible power production. For the applications considered here, CHF can be defined as a sudden temperature rise of the heater when a certain heat flux is reached. There are however several different mechanisms that may cause this temperature rise depending on the flow conditions. In a boiling water reactor (BWR) that operates with relatively high steam quality CHF is usually termed dryout and occurs when the thin water film on the heater rods evaporates and leaves the surface in direct contact with the vapor phase.

Even though this basic mechanism is known and a lot of effort has been spent on understanding the governing phenomenon, the most common way of predicting the dryout limit is still by empirical correlations. Such methods

TABLE 1. Nomenclature

Notation	Quantity	Dimension
d_h	Hydraulic diameter	[m]
C_p	Water heat capacity	[J/kg/K]
D	Deposition rate	[kg/m^2/s]
E	Entrainment rate	[kg/m^2/s]
G	Mass flux	[kg/m^2/s]
h_{lg}	Latent heat	[J/kg]
P	Wall perimeter	[m]
q''	Heat flux	[W/m^2]
W	Mass flow rate	[kg/s]
x	Steam quality	[-]
z	Axial height	[m]

Subscripts

Notation	Meaning
d	drop
f	film
v	vapor

can be highly accurate and reliable but they have some important drawbacks. First, a large number of expensive full-scale experiments are required to develop such correlations. Second, parameters that cannot be described by a single number cannot easily be correlated. The most important such parameter is probably the axial power distribution. It is known that shifting the power towards the outlet, where the steam quality is high, reduces the dryout limit. Most empirical correlations fail to accurately predict this effect; in fact, the whole correlation concept breaks down for parameters that are described by space dependent functions.

This situation and an increasing need for accurate dryout predictions as the reactor fuels become more optimized, has promoted an increased interest in phenomenological dryout modeling. In such models equations for the amount of film on the heated walls are formulated and solved. The main goal is of course to correctly predict the dryout power, but to be sure that a model really captures the mechanism of the dryout phenomenon it should be compared to direct measurements of the liquid film. One should here consider the difference between the film thickness and the film flow rate. They are of course related, e.g. by the triangular relationship (Hewitt G. F. in Hetsroni (1982)), but not equivalent. The film thickness has been measured with needle probes (Neal and Bankoff 1963), (Würtz 1978) and with conductance probes, (Collier and Hewitt 1964).

In most phenomenological dryout models, however, the mass flow rate of film plays a central role and should thus be of greater interest to the dryout research. To measure the film flow rate it is almost inevitable to extract the film from the flow. Such measurements have successfully been carried out by several groups by extracting the film through a porous wall section. Whalley et al. (1973) presented such measurements for air-water systems. In low pressure steam-water systems the film flow has been measured under adiabatic conditions (Hewitt and Pulling 1969) as well as diabatic condition (Hewitt et al. 1965). Singh et al. (1969) performed measurements in a high pressure steam-water system. The mentioned experiments were made in round tubes but the same technique has been applied to annular test section (Mannov 1973) and even small rod bundles (Gustafsson 1973). Bennett et al. (1966) presented a series of measurements where they used an axial power distributions with cold patches (i.e. unheated wall segments), which offered the first explanation of the influence of the axial power distribution on the liquid film flow rate and dryout power. The aim of the present study is to further investigate the influence of the power distribution at conditions typical for a boiling water reactor (BWR). For this purpose four axial power distributions were studied and the film flow rate was measured at several axial locations using the same extraction technique as mentioned above.

2. Measurements

2.1. *Experimental Setup*

The experiments presented here were performed in the high-pressure two-phase flow loop at the Royal Institute of Technology in Stockholm, Sweden. The objective of the experimental program was to measure the liquid film flow rate under conditions typical for a BWR. In particular the goal was to obtain data for realistic axial power distributions and to perform measurements at several axial locations to make direct comparison with solutions obtained from phenomenological models possible. Round tube geometry was chosen because of its simplicity compared to annular geometry or rod bundles. The film flow was measured by extracting the film through a porous wall section placed close to outlet of the test-section. The vapor content in the extracted sample was determined by condensing the sample in a heat exchanger and carefully monitoring the temperatures and flow rates at both the primary and secondary sides. The vapor content can then be calculated by a heat balance over the heat exchanger as:

$$x_s = \frac{W_2 \left(h_{2out} - h_{2in}\right) + W_1 \left(h_{out} - h_{sat}\right)}{W_1 h_{lg}} \tag{1}$$

where W_1 and W_2 are the flow rates at the primary and secondary side of the heat exchanger, respectively and h_{out} is the enthalpy at the outlet of the primary side. h_{2out}, h_{2in}, h_{sat} and h_{lg} are respectively the enthalpies at the

TABLE 2. Dimensions of test section and measurement system

Heated length of test section	3.65 m
Tube inner diameter	13.9 – 14.1 mm
Length of extraction unit	25 mm
Distance from end of heated length to extraction point	30 mm

outlet and inlet of the secondary side, the saturation enthalpy and the latent heat of vaporization.

In order to determine the liquid film flow rate the extracted sample flow, W_1, was increased from a low value – lower than the liquid film flow – in steps until vapor was detected in the sample. At that point it was assumed that the film flow rate was found. When the sample flow was increased even more, the liquid content stayed approximately constant and only the vapor flow in the sample increased. If the sample vapor content, x_s, is plotted against the extracted liquid flow rate, $(1 - x_s)W_1$, an L-shaped curved emerges, where the film flow rate can be determined, see Fig. 1.

A sketch of the loop and the film flow measurement system is shown in Fig. 2. Dimensions of the test section and important parts of the loop and measurement system are summarized in Table 2. The test sections were manufactured from stainless steel and heated electrically and the power distribution was imposed by varying the outer diameter of the tube. In order to change the axial location of the film measurement point it was necessary the dismount the test section and cut the tube. This was a time consuming but robust procedure. An exception was the uniform power distribution where the effective measurement point could be moved by changing the inlet temperature, thereby moving the onset of boiling but preserving all other parameters. In order to reproduce the same conditions in the loop after a movement of the measurement point, the local heat flux should be conserved after cutting the pipe (the local heat flux was for this purpose measured as the voltage over a segment of the test section). Note that for non-uniform power distributions, this implies a change in the average heat flux.

2.2. *Experimental Matrix*

In order to reduce the number of runs all experiment were carried out at 7 MPa pressure and 10 K inlet subcooling, which corresponds to normal operating conditions of a BWR. The mass flux was varied in three steps from 750 to 1750 kg/m^{2}s. Four different power distributions, as shown in Fig. 3, were used - uniform, inlet peak, middle peak and outlet peak. Each power distribution

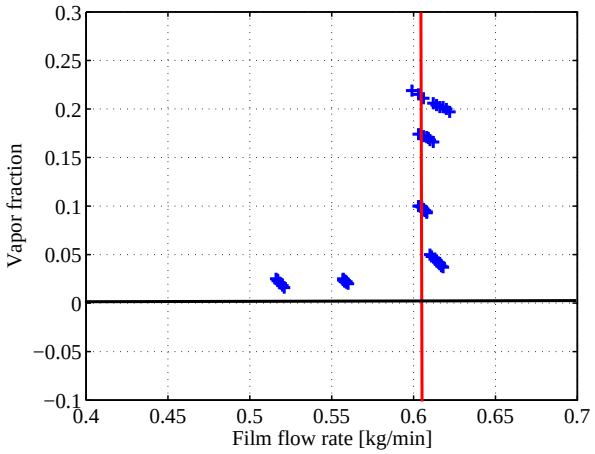

FIGURE 1. Example of suction curve from the experiments. The film flow rate is detmined from the intersection of the vertical part of the curve with the horizontal axis.

(except the uniform one) was run at two different power levels; one just slightly lower than the corresponding dryout power and one at reduced power, which was the same for all power distributions. In this way it was possible to study the film flow close to the dryout conditions but also to compare the power distributions at the same total power and flow conditions. For each set of boundary conditions the film flow was measured at 7 axial locations, the last one being located 80 cm from the outlet. Further upstream measurements were not possible because of very thick and ill-defined films and limited capacity of the heat exchanger and flow meter. The experimental matrix is summarized in Table 3.

3. Accuracy and Uncertainties

The accuracy of the measurements is important since the influence of the axial power distribution in a tube is quite small. Several sources of uncertainty can be identified. Obviously, all measurements of temperatures and flow rates will be associated with some uncertainty. These can be analyzed be differentiating

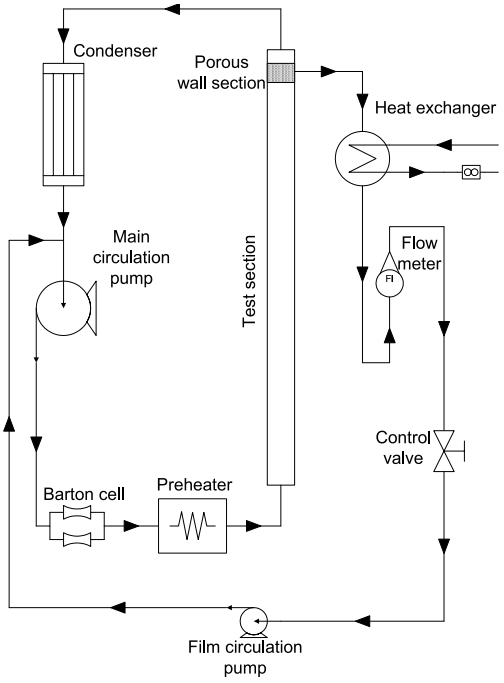

FIGURE 2. Sketch of the loop.

equation (1), which gives:

$$\frac{\partial W_f}{\partial W_1} = 1 + \left(\frac{h_{sat} - h_{out}}{h_{lg}} \right) \approx 2 \tag{2}$$

$$\frac{W_2}{W_1} \frac{\partial W_f}{\partial W_2} = -\left(\frac{h_{sat} - h_{out}}{h_{lg}} + x_s \right) \approx -1 \tag{3}$$

$$\frac{1}{W_1} \frac{\partial W_f}{\partial T_{out}} = \frac{C_p}{h_{lg}} \approx 0.003 \frac{1}{\mathrm{K}} \tag{4}$$

$$\frac{1}{W_1} \frac{\partial W_f}{\partial T_{2out}} = -\frac{1}{W_1} \frac{\partial W_f}{\partial T_{2in}} = -\frac{W_2}{W_1} \frac{C_p}{h_{lg}} \approx -0.06 \frac{1}{\mathrm{K}} \tag{5}$$

The numerical values were obtained by substituting typical values from the experiments into the equations. Since several thermocouples were used to measure the same temperatures at the heat exchanger it was possible to directly estimate the accuracy of the temperature measurements to ± 0.5 K. From equations (4) and (5) we can conclude that the uncertainty in temperatures at the

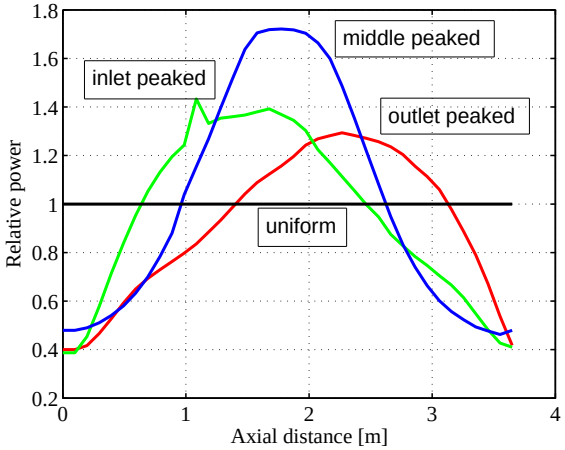

FIGURE 3. The four axial power distributions used in the experiments. The spike in the inlet peaked distribution is a manufacturing fault.

secondary side gives an error of about 3% in the film flow and that uncertainties in the temperatures at the primary side have negligible influence. The flow meter on the secondary side was verified several times to be accurate within 2%, which according to equation (3) translates to about 2% error in the film flow rate. The largest uncertainty is due to the flow meter on the primary side. When calibrated it showed a standard deviation of about 4%, giving 8% in W_f according to equation (2), but at low flow rates the accuracy was worse. As an estimate it was assumed that the error in the flow meter readings was ± 0.05 kg/min independent of the actual flow, which gives an error of ± 0.1 kg/min in W_f.

There are also possible systematic errors that must be considered. Singh et al. (1969) studied the influence of the length of porous wall segment and recommended to use a length of 1 in., which is very close to what was used in the present study. Another obvious issue is the possibility of redeposition of drops on the wall after the heated length but before the extraction point and possible condensation in the pipe before the heat exchanger. However, since the distances involved are very short – just three centimeters between the end of the heated length and the extraction point – and all pipes were well insulated, it is unlikely that these mechanisms would give any noticeable effect. In the same way heat losses from the heat-exchanger can be ruled out as negligible since the heat-exchanger was kept well insulated and the outer surface was in contact only with the cold secondary flow.

TABLE 3. Matrix of experiments. The reported dryout quality was measured in the loop for each pipe and mass flux before the film measurement begun. The pressure and inlet subcooling was 7 MPa and 10 K, respectively, for all measurements.

Mass flux $\frac{\text{kg}}{\text{min}}$	Profile	Outlet Quality[%]	Dryout Quality[%]
750	uniform	75	77
1250	uniform	51	54
1750	uniform	43	45
750	outlet	72	75
750	outlet	65	75
1250	outlet	50	54
1250	outlet	45	54
1750	outlet	40	43
1750	outlet	36	43
750	middle	74	77
750	middle	65	77
1250	middle	51	55
1250	middle	45	55
1750	middle	40	43
1750	middle	36	43
750	inlet	76	79
750	inlet	65	79
1250	inlet	52	57
1250	inlet	45	57
1750	inlet	43	46
1750	inlet	36	46

The possibility of heat losses in the main test section should also be considered. This was tested with subcooled flow by comparing the applied electrical power with the heat balance calculated from temperature measurements at the inlet and outlet of the test section. The discrepancy that was obtained by this method was always less than 5% and would not directly influence the film measurements. It would give a corresponding bias error to the reported steam quality though (no correction for this has been applied).

The largest uncertainty as well as source of systematic errors was probably the interpretation of the suction curves. As can be seen in Fig. 4 the curves do not always have a well defined vertical part. This type of curves are not unexpected since it is known that the liquid film carries disturbance waves, which will make the interface between the film and water phases fuzzy. Consistently

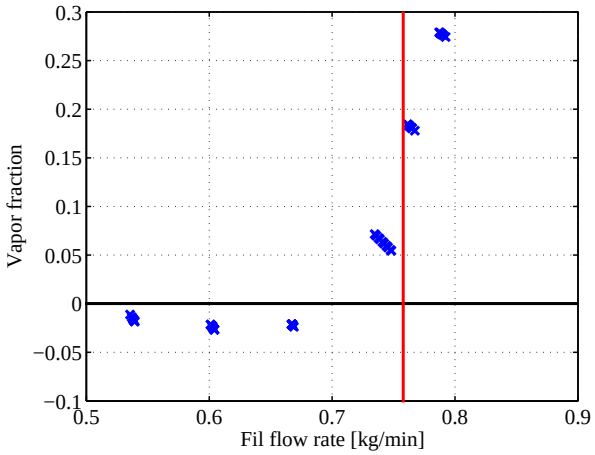

FIGURE 4. Example of a suction curve from the experiment where the film is not well defined. The reason is probably large disturbance waves on the film surface.

with this explanation this type of curves were more common when the film was thick, i.e. for relatively high film flow rates. A few curves showed a negative slope as in Fig. 5. This behavior seems difficult to explain and must probably be considered as an inaccuracy of the measurement equipment.

Based on the above consideration it was concluded that main error sources were the accuracy of the flow meter on the primary side of the heat exchanger and the interpretation of the suction curves. When the suction curves were reasonably sharp and readily interpreted the error was estimated to be within ± 0.1 kg/min. In the cases of less well defined curves the error-bounds were increased to ± 0.2 kg/min.

4. Results

The results of all measurements are shown in Tables 4 and 5. In Fig. 6 the results from the measurements on the uniform power distribution are shown. As can be seen the film flow rate extrapolates almost to zero when the dryout power is approached. This is consistent with the results reported by Hewitt et al. (1965).

Since the difference between the power distributions is small it is easier to see if one considers the drop flow curves rather than the film flow itself. For this purpose the drop flow rate can be calculated as $W_d = W - W_v - W_f$, where W, W_v are the total flow rate and the flow rate of vapor, respectively. In Figs. 7 and 8 the drop flow distributions of the inlet and outlet peaked profiles, at the same total power, are shown. It is clear that the inlet peaked profile leaves

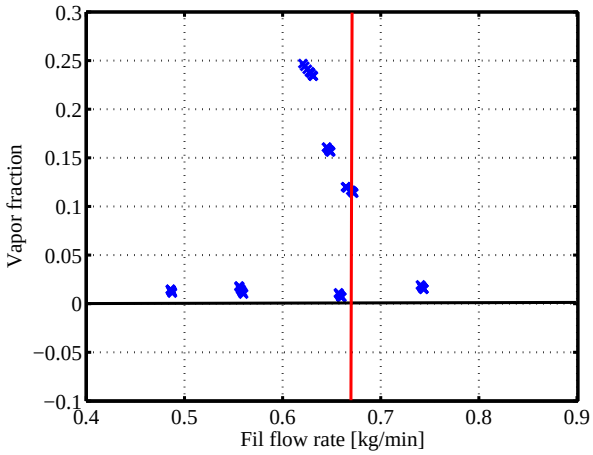

FIGURE 5. Example of suction curve from the experiment with negative slope. This behavior was rare, but no physical explanation could be found. It should be considered as an inaccuracy of the measurement equipment.

less entrained drops and thus more film, which is consistent with the trend observed for the dryout power, i.e. that the margin to dryout is larger for the inlet peaked distribution. The results of the middle peaked power distribution are not shown in these figures since the results were so close to the inlet peaked profile that it is within the uncertainty of measurements.

The current results are consistent with investigations performed by Bennett et al. (1966) who used a cold patch on a otherwise uniformly heated tube to elucidate the influence of the axial power distribution on the liquid film flow and dryout power. Their and the present results indicate that in channels with outlet-peaked axial power distributions the flow rate of entrained drops is higher than in the case with the inlet-peaked profile. This brings about a thinner liquid film in the exit part of the channel, which eventually leads to earlier dryout in the former case. The mechanism behind this effect is hydrodynamical; the part of the channel with large film flow, where the entrainment dominates over the deposition, is shorter in a channel with inlet-peaked power distribution.

Fig. 9 and 10 show a comparison of the present measurements with two phenomenological models of annular flow. Both models are based on the following simple mass balance equation for the liqud film:

$$\frac{1}{P}\frac{dW_f}{dz} = D - E - \frac{q''}{h_{lg}} \tag{6}$$

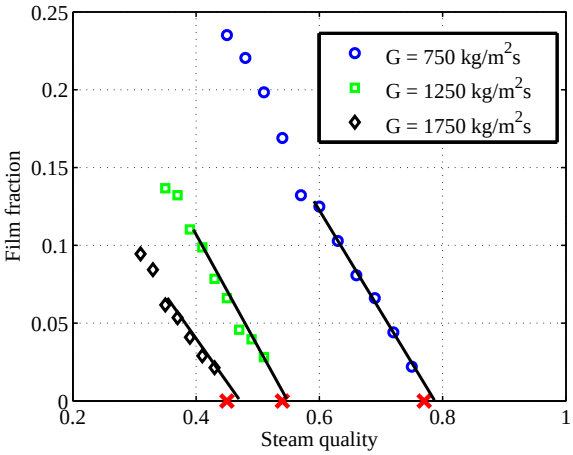

FIGURE 6. Film fraction against steam quality for the uniform power distribution, for three different flow rates. Note that the film flow rate extrapolates almost to zero as the dryout point (red cross) is approached.

where D and E denote the deposition and entrainment rates of drops and q'' is the wall heat flux. The two models considered here were presented by Hewitt and Govan (1990) and Okawa et al. (2003) ,respectively. The boundary condition at the beginning of annular flow from the latter model was applied also to the first, since the authors did not provide the boundary conditions in that case. As can be seen in the figures the agreement between models and experiment is excellent. It should be kept in mind however that these models were developed for round tube geometry similar to the one used here. In another geometric configuration, such as a rod-bundle or annulus, the accuracy can be expected to be worse. It is also of interest to note that the flow rate of drops is almost constant along the channel and that the boundary condition at the beginning of annular flow thus is very important at the present channel length.

5. Conclusions

The film flow rates has been measured in heated round tubes with various axial power distributions at conditions typical to what is found in a BWR. In agreement with earlier measurements it was observed that, within the accuracy of the measurements, the film flow rate approaches zero as the dryout power is approached. Furthermore it is concluded that the known trend in the dryout power, i.e. that inlet peaked power distributions result in higher dryout power than outlet peaked ones, is reflected by a consistent trend in the film

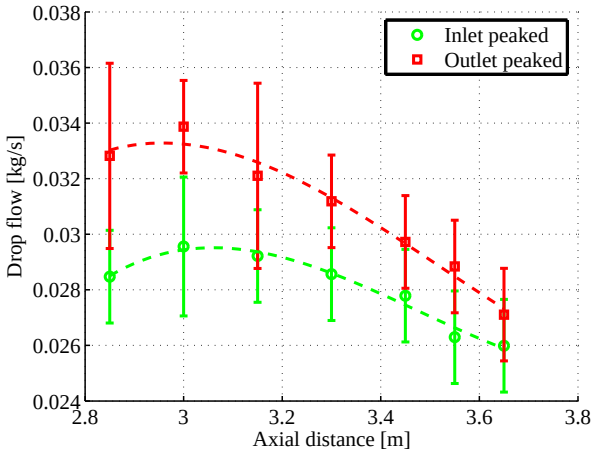

FIGURE 7. Drop flow versus axial distance for inlet- and outlet-peaked axial power distributions. Mean heat flux $q'' = 0.74\,\mathrm{MW/m^2}$, mass flux $G = 750\,\mathrm{kg/m^2s}$, pressure $p = 7\,\mathrm{MPa}$, inlet subcooling 10 K.

flow measurements. Finally it was shown that the measurements are in good agreement with two phenomenological models presented by Okawa et al. (2003) and Hewitt and Govan (1990).

6. Acknowledgments

The financial support provided by the Swedish Center for Nuclear Technology (SKC) is gratefully acknowledged. The authors would like to express their appreciation to S. Hedberg and P. Persson for their assistance in performing the experiments.

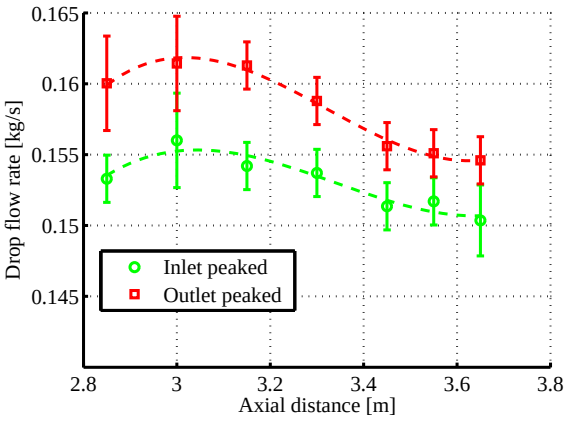

FIGURE 8. Drop flow versus axial distance for inlet- and outlet-peaked axial power distributions. Mean heat flux $q'' = 1.00$ MW/m^2, mass flux $G = 1750$ kg/m^{2}s, pressure $p = 7$ MPa, inlet subcooling 10 K.

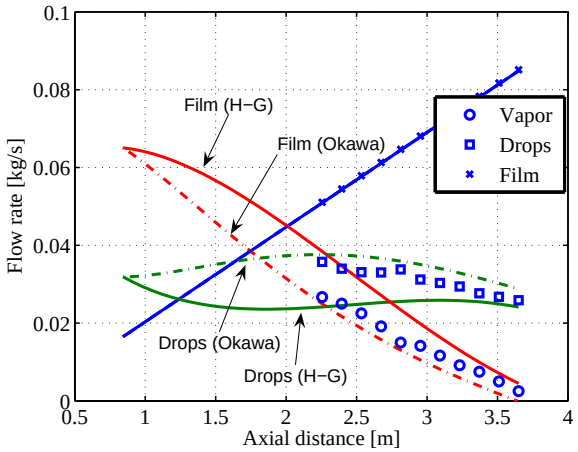

FIGURE 9. Comparison of measured flow rates with predictions by Hewitt and Govan (1990) and Okawa et al. (2003) models. Uniform axial power distribution, mean heat flux $q'' = 0.84$ MW/m^2, mass flux $G = 750$ kg/m^{2}s, pressure $p = 7$ MPa, inlet subcooling 10 K.

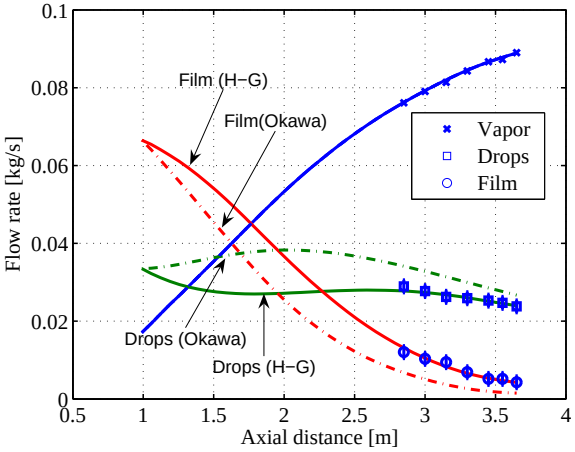

FIGURE 10. Comparison of measured flow rates with predictions by Hewitt and Govan (1990) and Okawa et al. (2003) models. Inlet-peaked axial power distribution, mean heat flux $q'' = 0.86$ MW/m^2, mass flux $G = 1750$ kg/m^{2}s, pressure $p = 7$ MPa,inlet subcooling 10 K.

TABLE 4. Results of film measurements with uniform power distribution. The axial position, z, is given in meters and the film flow rate, W_f, is given in kg/min.

G	$750\frac{\text{kg}}{\text{m}^2\text{s}}$		$1250\frac{\text{kg}}{\text{m}^2\text{s}}$		$1750\frac{\text{kg}}{\text{m}^2\text{s}}$	
x	75%		51%		43%	
	z	W_f	z	W_f	z	W_f
	3.65	0.15	3.65	0.32	3.65	0.34
	3.51	0.3	3.52	0.45	3.49	0.46
	3.37	0.45	3.39	0.52	3.34	0.65
	3.23	0.55	3.25	0.75	3.18	0.85
	3.09	0.7	3.12	0.89	3.02	0.98
	2.95	0.85	2.99	1.12	2.86	1.34
	2.81	0.9	2.86	1.25	2.71	1.5
	2.67	1.15	2.72	1.5	-	-
	2.53	1.35	2.59	1.55	-	-
	2.39	1.5	-	-	-	-
	2.26	1.6	-	-	-	-

TABLE 5. Results of measurements with non-uniform power distribution. The axial position, z, is given in meters and the film flow rate, W_f, is given in kg/min. Measurements with a * are accurate within ±0.2 kg/min and the rest within ±0.1 kg/min.

G	$750\frac{\text{kg}}{\text{m}^2\text{s}}$		$1250\frac{\text{kg}}{\text{m}^2\text{s}}$		$1750\frac{\text{kg}}{\text{m}^2\text{s}}$	
	Outlet peaked					
x	72%	65%	50%	45%	40%	36%
z	W_f	W_f	W_f	W_f	W_f	W_f
3.65	0.3	0.75	0.5	0.9	0.6	1.05
3.55	0.3	0.75	0.55*	0.95	0.55	1.1
3.45	0.55*	0.8	0.6	1.0	0.65*	1.15
3.3	0.5*	0.85	0.75	1.1	0.75*	1.2
3.15	0.7*	1.0*	0.8*	1.25	0.8	1.4
3.0	0.85	1.1	0.9	1.5	0.95	1.6*
2.85	1.0	1.4*	1.25*	1.9*	1.6	2.0*
	Middle peaked					
x	74%	65%	51%	45%	40%	36%
z	W_f	W_f	W_f	W_f	W_f	W_f
3.65	0.3	0.8	0.65	1.15	0.75	1.2
3.55	0.35	0.85	0.6	1.1	0.65	1.2
3.45	0.35	0.8	0.6	1.1	0.65	1.4
3.3	0.4	0.9	0.65	1.3*	0.8	1.65*
3.15	0.45	0.95	0.6	1.3*	0.8	1.65*
3.0	0.55	1.1	0.78	1.4	0.85	1.7
2.85	0.65	1.25	0.95	1.85	1.05	2.0
	Inlet peaked					
x	76%	65%	52%	45%	43%	36%
z	W_f	W_f	W_f	W_f	W_f	W_f
3.65	0.3	0.85	0.6	1.05	0.65	1.3*
3.55	0.35	0.9	0.6	1.05	0.65	1.3
3.45	0.35	0.88	0.6	1.08	0.65	1.4
3.3	0.4	0.95	0.7	1.22	0.7	1.4
3.15	0.45	1.0	0.75	1.3*	0.8*	1.55
3.0	0.55	1.15*	0.85	1.4*	0.85	1.65*
2.85	0.65	1.35	1.0	1.8	0.95*	2.0

References

A. W. Bennett, G. F. Hewitt, H. A. Kearsey, R. K. F. Keeys, and D.J. Pulling. Studies of burnout in boiling heat transfer to water in round tubes with non-uniform heating. Technical Report R5076, AERE, 1966.

J. G. Collier and G. F. Hewitt. Film thickness measurement. *ASME paper 64–WA/HT–41*, 1964.

B. Gustafsson. Two-phase flow in a nine-rod bundle with tilted power distribution. preliminary flow split and film flow measurements. In *European Two-Phase Flow Group Meeting*, Jun 1973.

G. Hetsroni. *Handbook of Multiphase Systems*. Hemisphere Publisher Corporation, 1982. ISBN 0-07-028460-1.

G. F. Hewitt and A. H. Govan. Phenomenological modelling of non-equlibrium flows with phase change. *Int. J. Heat and Mass Transfer*, 33(2):229–242, 1990.

G. F. Hewitt and D. J. Pulling. Liquid entrainment in adiabatic steam-water flow. Technical Report R5374, AERE, 1969.

G. F. Hewitt, H. A. Kearsey, P. M. C. Lacey, and D. J. Pulling. Burnout and film flow in the evaporation of water in tubes. Technical Report R4864, AERE, 1965.

G. Mannov. Film flow measurements in concentric annulus 3500 x 27.2 x 17 mm with heated and unheated rod. Technical Report SDS-65, Risø National Laboratory, 1973.

L. G. Neal and S. G. Bankoff. A high resolution resistivity probe for determination of local void properties in gas-liquid flow. *AIChE Journal*, 9, 1963.

T. Okawa, A. Kotani, I. Kataoka, and M. Naito. Prediction of Critical Heat Flux in Annular Flow Using a Film Flow Model. *Journal of Nuclear Scince and Technology*, 40(6):388–396, June 2003.

K. Singh, C. C. Pierre, W. A. Crago, and E. O. Moeck. Liquid Film Flow-Rate in Two-Phase Flow of Steam and Water at 1000Lb/Sq.In.Abs. *AIChE Journal*, 15 (1), 1969.

P. B. Whalley, G. F. Hewitt, and P. Hutchinson. Experimental wave and entrainment measurements in vertical annular two-phase flow. Technical Report R5374, AERE, 1973.

J. Würtz. An Experimental and Theoretical Investigation of Annular Steam-Water Flow in Tube and Annuli at 30 to 90 bar. Technical Report 372, Risø National Laboratory, 1978.